31 MAR 1989

AFOSR-TR- 89-0531

HIGHLY ORIENTED FIBER REINFORCED CERAMIC COMPOSITES

1 August 1988 - 31 January 1989

FINAL REPORT

31 March 1989

CPS 89-004

CERAMICS PROCESS SYSTEMS

HIGHLY ORIENTED FIBER REINFORCED CERAMIC COMPOSITES

1 August 1988 - 31 January 1989

FINAL REPORT

31 March 1989

CPS 89-004

Contract F49620-88-C-0104

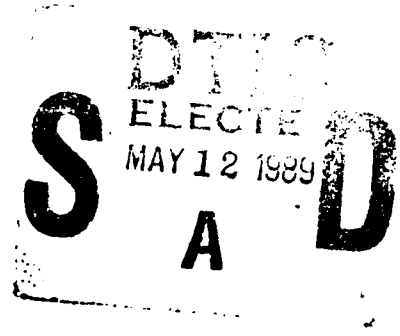

Prepared by

Ceramics Process Systems Corp.
840 Memorial Drive
Cambridge, MA 02139

Prepared for

Air Force Office of Scientific Research
Building 410
Bolling Air Force Base, DC 20332-6448

UNCLASSIFIED

SECURITY CLASSIFICATION OF THIS PAGE UNCLASSIFIED

REPORT DOCUMENTATION PAGE

Form Approved OMB No. 0704-0188

1a. REPORT SECURITY CLASSIFICATION: UNCLASSIFIED	1b. RESTRICTIVE MARKINGS: N/A
2a. SECURITY CLASSIFICATION AUTHORITY: N/A	3. DISTRIBUTION/AVAILABILITY OF REPORT: Approved for public release. Distribution unlimited.
2b. DECLASSIFICATION/DOWNGRADING SCHEDULE: N/A	
4. PERFORMING ORGANIZATION REPORT NUMBER(S): CPS 89-004	5. MONITORING ORGANIZATION REPORT NUMBER(S): AFOSR-TR- 89-0531
6a. NAME OF PERFORMING ORGANIZATION: Ceramics Process Systems Corp. / 6b. OFFICE SYMBOL (If applicable): N/A	7a. NAME OF MONITORING ORGANIZATION: Air Force Office of Scientific Research
6c. ADDRESS (City, State, and ZIP Code): 840 Memorial Drive, Cambridge, MA 02139	7b. ADDRESS (City, State, and ZIP Code): Building 410, Bldg, Bolling AFB, DC 20332-6448
8a. NAME OF FUNDING/SPONSORING ORGANIZATION: AFOSR / 8b. OFFICE SYMBOL (If applicable): NA	9. PROCUREMENT INSTRUMENT IDENTIFICATION NUMBER: F49620-88-C-0104
8c. ADDRESS (City, State, and ZIP Code): same as 7b.	10. SOURCE OF FUNDING NUMBERS: PROGRAM ELEMENT NO. 61102F; PROJECT NO. 3005; TASK NO. A1; WORK UNIT ACCESSION NO.

11. TITLE (Include Security Classification)

Highly Oriented Fiber Reinforced Ceramic Composites (U)

12. PERSONAL AUTHOR(S)

Ran-Rong Lee

13a. TYPE OF REPORT	13b. TIME COVERED	14. DATE OF REPORT (Year, Month, Day)	15. PAGE COUNT
Final	FROM 8/1/88 TO 1/31/89	3/31/89	66

16. SUPPLEMENTARY NOTATION

N/A

17. COSATI CODES			18. SUBJECT TERMS (Continue on reverse if necessary and identify by block number)
FIELD	GROUP	SUB-GROUP	Ceramic composites, Aluminum nitride, Silicon carbide. (JES)

19. ABSTRACT (Continue on reverse if necessary and identify by block number)

Highly dense SiC-AlN alloys having unique microstructures and a fracture toughness up to 6 $MPam^{1/2}$ were successfully produced by pressureless sintering of commercially available SiC and AlN powders. Appropriate sintering aids, sintering temperatures, sintering period and sintering conditions were identified. The sintered SiC-AlN alloys can achieve a single phase solid solution after an appropriate thermal treatment. The lattice constants of the solid solution varied linearly with SiC/AlN ratio. Optimized annealing yielded decomposition of the solid solution and formed a unique microstructure, which was composed of equiaxed grains with modulated features, heavily faulted elongated grains and very clean grain boundaries. The ratio of the equiaxed grains and elongated grains in the alloys can be controlled by the ratio of AlN and SiC. The preliminary mechanical testing results showed that the alloys with duplex microstructure can have fracture toughness up to 6 $MPam^{1/2}$, almost twice that of pure SiC.

20. DISTRIBUTION/AVAILABILITY OF ABSTRACT	21. ABSTRACT SECURITY CLASSIFICATION
☒ UNCLASSIFIED/UNLIMITED ☐ SAME AS RPT ☐ DTIC USERS	UNCLASSIFIED
22a. NAME OF RESPONSIBLE INDIVIDUAL: [redacted] (COL KEN K. HAYES)	22b. TELEPHONE (Include Area Code): (202) 767-0463 / 22c. OFFICE SYMBOL: N/A

DD Form 1473, JUN 86 *Previous editions are obsolete.* SECURITY CLASSIFICATION OF THIS PAGE

UNCLASSIFIED

FOREWORD

This document, submitted by Ceramics Process Systems, is the final report for the Highly Oriented Fiber Reinforced Ceramic Composites Phase I program. The program was conducted for the Air Force Office of Scientific Research under Contract F49620-88-C-0104. The research proposal was submitted under the SBIR FY 1988 in response to Air Force SBIR #AF88-237 and #AF88-112. This report covers the period from 1 August 1988 through 31 January 1989.

This research received assistance from the High Temperature Materials Laboratory (HTML) at Oak Ridge National Laboratory (ORNL) through their User Research Program. This program permits industry and universities to use their special research equipment for characterizing the microstructure and microchemistry of materials and to correlate their physical and mechanical properties.

The research on the new alloys production, including work on alloy formulation, raw materials preparation, sintering aids for pressureless sintering and firing, and part of the analytical work was done at Ceramics Process Systems. Some of the characterizations required advanced and special instruments; these characterizations were performed by a CPS researcher at HTML.

Special thanks are due to the committee of the User Center at the HTML which allowed us to use advanced analytical equipment and to the following who assisted us in the operation of the instruments, especially to Dr. C. Hubbard, Mr. B. Cavin, and Ms K. More.

CONTRIBUTORS TO THIS REPORT

Dr. Ran-Rong Lee, Principal Investigator
Dr. James D. Hodge, Former Principal Investigator
Dr. Wen-Cheng James Wei
Dr. John Halloran
Ms Frances Schutzberg

ABSTRACT

Highly dense SiC-AlN alloys having unique microstructures and a fracture toughness up to 6 $MPam^{1/2}$ were successfully produced by pressureless sintering of commercially available SiC and AlN powders. Appropriate sintering aids, sintering temperatures, sintering period and sintering conditions were identified. The sintered SiC-AlN alloys can achieve a single phase solid solution after an appropriate thermal treatment. The lattice constants of the solid solution varied linearly with SiC/AlN ratio. Most of the phase for assisting liquid phase sintering was trapped inside the SiAlCN grains and was fully crystallized. Optimized annealing yielded decomposition of the solid solution and formed a unique microstructure, which was composed of equiaxed grains with modulated features, heavily faulted elongated grains and very clean grain boundaries. The ratio of the equiaxed grains and elongated grains in the alloys can be controlled by the ratio of AlN and SiC. The preliminary mechanical testing results showed that the alloys with duplex microstructure can have fracture toughness up to 6 $MPam^{1/2}$, almost twice that of pure SiC, and comparable to monolithic or whisker-reinforced Si_3N_4.

TABLE OF CONTENTS

LIST OF FIGURES

LIST OF TABLES

SECTION 1

OBJECTIVES

Whisker reinforced ceramics have shown better mechanical properties than monolithic ceramics; However, progress in engineering acceptable whisker reinforced composites has been retarded by processing problems, such as incomplete densification because of the presence of non-sinterable whiskers. Normally hot pressing or hot isostatic pressing (HIP) is required to achieve high density and good property, but both are expensive methods and hot pressing only can produce simple geometry parts. Another important problem related to the processing of whisker reinforced composites is the safety and health issue during handling whiskers.

The goal of this research program is to fabricate ceramic-ceramic alloys reinforced with whisker-like feature which are grown in situ during sintering and annealing of the ceramic matrix. A process is proposed that involves the pressureless densification of AlN-SiC alloys at high temperature and then the controlled growth of whisker-like or platlet-like precipitates from the solid solution at temperatures within the miscibility gap of the AlN-SiC alloys.

Three major objectives were proposed for Phase I of this research:

1) Raw materials selection and/or preparation.

2) Identification of additives required to pressureless sinter the solid solution.

3) Elucidation of thermal profiles required to form and, subsequently, decompose the solid solution.

SECTION 2

SUMMARY OF REPORT

All the objectives proposed in Phase I (6 months) of this research project have been successfully achieved. Moreover, the alloys have shown unique microstructure and good mechanical properties after appropriate sintering and heat treatments. Following are the summary results related to each objective.

The process to prepare SiC-AlN alloys was evaluated and identified. The alloys can be prepared from commercially available SiC and AlN powders, which are inexpensive and adaptable to mass production. Both alpha and beta SiC powder can be used to prepare the alloy, although the alloys prepared from alpha SiC can have better density at lower temperatures. The green body of these alloys can be prepared by conventional ceramic processing, such as slip casting, pressure casting, and dry pressing. Then the green body can be pressureless sintered to high density.

The sintering aid required to assist pressureless sintering has also been studied and yttria sintering aid was found to be better than alumina and calcia. Only 2 wt% of yttria was required to obtain high density. Different alloys have different optimum sintering temperatures for achieving high density. The alloys with higher AlN content can be densified at lower sintering temperature, but all the alloys can achieve high density at 2050 to

2100°C. The mechanism for densification was proposed to be liquid phase sintering.

After sintering, the highly dense SiC-AlN alloys could achieve single solid solution phase after solution treatment at temperatures above 2225°C. The alloys after solid solution treatment had equiaxed grains with 2H structure, and the lattice constants of the solid solution varied linearly as the SiC/AlN ratio changed. Most of the yttrium-rich phase was trapped inside the SiAlCN grains and was fully crystallized.

Optimum annealing at 1860°C yielded decomposition of the solid solution and formed a unique microstructure, which was composed of equiaxed grains with modulate feature, elongated grains with heavy faulting and clean grain boundaries. The equiaxed grains were found to have 2H structure and contain more AlN. The elongated grains had other polytypes, such as 6H and 3C and contain less than 10% AlN. The ratio of the equiaxed grains and elongated grains in the alloys can be controlled by the ratio of AlN and SiC. The alloys with duplex microstructure are believed to have good fracture toughness by crack deflection at the elongated grains and high temperature creep resistance through retarding grain boundary sliding and dislocation movement. The preliminary mechanical testing results demonstrated that the alloys can have a fracture toughness up to 6 $MPam^{1/2}$, almost twice that of pure SiC and comparable to monolithic or whisker reinforced Si_3N_4.

SECTION 3

LITERATURE REVIEW

AlN-SiC ceramics have been studied for the past decade[1-16] because of their potential application at high temperature. Several different methods were used to prepare AlN-SiC composite powders. The first method is the mechanical mixing of commercially available SiC and AlN powders[3]. The second method is the carbon-thermal reduction of synthetic silica and alumina,[1,2] and the third is mixing Si_3N_4 and Al_4C_3 powder.[5] The carbon thermal reduction could yield a smaller particle size and better mixing, but the purity of the alloy powder and the production scale were limited. The $Si_3Al_4N_4C_3$ solid solution had been successfully prepared from Si_3N_4 and Al_4C_3 powder, but the range of the solid solution was limited by their ratio. The mechanical mixing of commercial SiC and AlN powder for preparing AlN-SiC is easy and straightforward. However, different SiC powders affected the formation of the SiC-AlN solid solution,[8,10] and the various particle sizes of SiC and AlN powders were also critical for the formation of the solid solution.[8]

After the ceramic powders were prepared and mixed, hot-pressing was commonly used to consolidate the alloy to high density.[2-4,6-15]. Sometimes boron was used as a sintering aid during hot pressing,[2] but usually boron was not required.[3-4,6-15]. Typical density of the hot-pressed alloys was 3.08 gm/ml, close to the theoretical density. The hot pressing

method is expensive and can only produce simple geometric shapes. Although pressureless sintering is better in both aspects, but it is not easy to obtain fully dense composites. Not much work has been done on the pressureless sintering of SiC-AlN alloys.[1-16] Huang et al[13] found out that with a minor amount of AlN, SiC-Al_2OC could be pressureless sintered to high density because of the liquid phase forming from Al_2O-SiC. A major objective of this current research is to determine appropriate sintering aids for the pressureless sintering of SiC-AlN.

Studies of the phase transformation of the alloys during sintering found that alloys containing beta-SiC would transform to 2H phase and some minor 6H and beta phases.[4,6] For alloys prepared from alpha-SiC, 2H and 6H would be the dominate phases, with 15R and 4H the minor phases. The mechanisms of 15R -> 2H and 4H -> 2H were suggested by Zangvil and Ruh to occur through a diffusion control process in a direction parallel to the basal planes.[15] The study of the AlN and SiC diffusion couple which was formed at 2200°C/8 hr found the following phase sequence: AlN - 2H (10 um thickness) - 4H (40 um thickness) - SiC. The composition changed abruptly from 26% AlN in the 2H layer to 11.3% AlN in the 4H layer. The authors also indicated that the alloys were near stoichiometry throughout the solid solution.

The temperature for achieving a single solid solution phase was not always the same in the literature.[3-15] Ruh and Zangvil[3] prepared AlN-SiC alloys from pure SiC and AlN powder and found that solid solutions of 2H structure formed in the alloys containing 35 to 100% AlN after hot-pressing at 2100°C. For the alloys containing less than 35% AlN, other polytypes such as 2H, 4H, 6H, 15R and 21R were found.

Rafaniello et al[4] prepared the alloys by using the powders produced from carbon-thermal reduction of silica and alumina. They also found that the materials with compositions between 15 and 75 wt% AlN were nonhomogeneous when hot pressed below 2100°C, and the miscibility gap was suggested. These results were quite different from their previously reported results[2], where a single solid solution phase was reported. Tsukuma et al[5] prepared the alloys from the mixture of Si_3N_4 and Al_4C_3 powders and had quite different results. They found that single phase $Si_3Al_4N_4C_3$ formed when firing the sample at 1800°C for 1 h under 10 MPa Ar gas pressure. Later Zangvil and Ruh[7,8] again found the difficulty of forming a single solid solution when they hot pressed the alloys. Even at 2100°C for 4 hrs, some inhomogeneous regions were still found. Kuo et al[14] further noticed that with beta-SiC powder it was relatively easy to form a 2H solid solution compared to using alpha-SiC powder, due to dissolution rate of these two materials into SiC-AlN-Al_2OC solid solution. However, Huang et al[13] indicated that there was no observable difference in the dissolution rate between beta and alpha SiC. Recently, Zangvil and Ruh[16] proposed a tentative SiC-AlN phase diagram, where 1900°C (the dotted line in the phase diagram) was suggested to be the solid solution temperature.

Long time annealing in the region of the miscibility gap was used to mature the growth of precipitates. Rafaniello et al[4] annealed the alloys which were prepared from carbo-thermal reduction of silica and alumina and found cellular-type precipitates in the alloys after annealing at 1700°C for 90 hrs. The microanalysis showed that the precipitates could have 93.4% AlN or 8% AlN. Kuo et al[10] subsequently showed that excess oxygen may accommodate the precipitation by forming of Al_3O_3N spinel in the SiC-Al_2OC-AlN

system. Different precipitation features were observed[14] when the alloys were prepared from pure SiC and AlN powders. Modulated features with 7 and 15 nm wavelength were observed after long annealing at 1650°C and 1900°C, respectively, and no other type of precipitate was found in the samples prepared from pure SiC and AlN powders. The spinodal decomposition was suggested to be the mechanism for the formation of modulated structures.

Several mechanical and physical properties corresponding to different compositions had been reported.[2,3]. Young's modulus and hardness were decreased and thermal expansion increased as AlN content increased. However, not much work has been done on the material containing precipitates.

SECTION 3

EXPERIMENTAL

3.1 Raw materials

Three different commercial SiC powders (two beta phase and one alpha phase) and one AlN powder were selected for study of SiC-AlN alloys. To achieve fully density through pressureless sintering, three oxides, yttria, alumina, and calcia were used as the sintering aid. The physical properties of these powders are listed in Tables 1 and 2.

Although the surface area of the three SiC powders are similar, about 15 m^2/gm, the density obtained from Lonza alpha-SiC and Superior Graphite beta-SiC is better than that obtained with Starck beta-SiC, as is discussed later.

3.2 Preparation of green specimen

A solution composed of iso-propanol, 2.5 wt%* EMCOL CC-55 (used as a dispersant) and 1 wt%* Elvacite 2046 (used as a binder) were pre-mixed for at least 4 hours. Then, the powders with the ratios shown in Table 3 were dispersed into the solution. The alloys had three different AlN/SiC ratios**: 7/3, 5/5 and 3/7. After tumbling the mixture for 16 hours, the well dispersed slurry was slip-cast in a plaster mold with dimensions of 15x15x10 mm.

---

* The wt% is based on the solid phase.
** The ratio is in weight, but it is very close to molar ratio because the densities of SiC and AlN are about the same.

TABLE 1 CHEMISTRY AND PROPERTIES OF AS-RECEIVED SiC AND AlN POWDERS

	AlN(*1)	SiC(*2)	SiC(*3)	SiC(*4)
Al	> 64%	<0.5%	0.04%	0.018%
N	33.1%	---	----	0.21%
Si	----	balance	balance	balance
C	0.07%	balance	30.54%	balance
O	2.0%	<1.0%	0.85%	0.8%
Free Si	----	<0.2%	----	0.03%
Free carbon		<0.5%		0.85%
Fe	0.018%	<0.1%	0.036%	0.016%
Ca	-----	--	0.002%	0.002%
other metal imp.	< 0.05%	--	------	
Sulfur		--		<0.5%
Average Size (um)	1.0	0.6±0.2	0.62	0.6
BET (m^2/gm)	5.1-5.2	15±1	15.5	15+

*1. AlN powder, grade C, Hermann C. Starck, Inc., New York 10017.
*2. Alpha-SiC powder, Carbogran UF-15, Lonza Inc, Engineered Materials, Jersey City, NJ 07304.
*3. Beta-SiC powder, B 10, Hermann C. Starck, Inc., New York 10017.
*4. Beta-SiC powder, HSC 059, Superior Graphite Co., Chicago, Il 60606.

TABLE 2 PROPERTIES OF SOME CHEMICALS USED AS SINTERING AIDS

1) Yttrium oxide finest, H. C. Starck

C_{tot} = 0.13%
FSSS = 0.28 micron
BET area = 14.15 m^2/g
Scott-density = 2.5 g/in^3

2) A16 alumina, Alcoa

3) Calcium Oxide, Cerac, Inc.

-325 mesh
99.99% pure

TABLE 3 THE FORMULATION (in wt%) OF AlN-SiC ALLOYS AND THE PACKING POWDERS (p.p.)

Sample	SiC (phase)	AlN	Sintering aids
AY2	49% (alpha)	49%	2% yttria
AY4	48% (alpha)	48%	4% yttria
BY2	49% (beta)*	49%	2% yttria
BY4	48% (beta)	48%	4% yttria
SBY2	49% (beta)**	49%	2% yttria
SBY4	48% (beta)	48%	4% yttria
73Y2	29.4% (alpha)	68.6%	2% yttria
37Y2	68,6% (alpha)	29.4%	2% yttria
AAY2	49% (alpha)	49%	1% yttria + 1% alumina
BAY2	49% (beta)**	49%	1% yttria + 1% alumina
AA2	49% (alpha)	49%	2% alumina
BA2	49% (beta)**	49%	2% alumina
AC2	49% (alpha)	49%	2% calcia
a-p.p.	50% (alpha)	50%	--
b-p.p.	50% (beta)*	50%	--

* Hermann C. Starck, Inc

** Superior Graphite Co.

The molded parts were dried at room temperature and then put into a 80°C oven to completely remove solvent.

Besides the mechanical mixing of AlN and SiC powders to prepare SiC-AlN alloys, other processes such as the sol-gel process also were preliminarily evaluated. However, because of the success of achieving high density and single solid solution phase by using commercial SiC and AlN powders and the limitation of production scale and cost of the sol-gel process, major efforts were placed on the preparation of SiC-AlN alloys through commercially available powders.

3.3 Sintering and heat treatment

A high temperature graphite furnace (Astro, a division of Thermal Technology Inc.) was used to densify and perform the annealing treatment. High purity argon gas with a pressure slightly higher than ambient atmosphere vented the furnace at 0.6 l/min flow rate. The samples were put in the graphite crucible, and sometimes buried with packing powder.

The sintering profile followed the schedule below:

room temperature to 250°C, 10°C/min

250 to 400°C, 3°C/min

hold at 400°C for 1 hr

400 to 1750°C, 20°C/min

1750 to sintering temperature, 10°C/min

hold at sintering temperature for 1 to 6 hr

sintering temperature to solid solution temperature, 10°C/min

hold at solid solution temperature for 1 to 6 hr

cooling in furnace, -40°C/min

The annealing between 1650 to 1860°C was conducted after the alloys were densified. Argon atmosphere and packing powder were always used during annealing to prevent the degradation of alloys.

3.4 Characterization

3.4.1 Optical microscopy and scanning electron microscopy

The sintered AlN-SiC alloys were ground and then polished by using various grades of diamond paste. After polishing, the samples were etched with Murakami's reagent and a fused salt mixture of KOH and KNO_3. The samples were then examined under the optical microscope and scanning electron microscope (SEM).

3.4.2 X-ray diffractometry

XRD analysis was conducted by using commercial equipment (Scitag Inc., Santa Clara, CA) at 45 KV and 40 mA. Normally the surface for scanning was cut and ground from the center of the samples. The scanning rate was 0.5°/min. For precise lattice constant measurement, the samples were ground into powder and then mixed with silicon powder (#640b, National Bureau of Standards) as an internal standard. The scanning rate was slowed down to 0.2°/min and the range was between 25 to 150°. The lattice constants were calculated by using computer software with least square fitting.

3.4.3 Transmission electron microscopy

The specimens were cut into 3-mm disks and polished down to 80 um thick. Then the thin foils were dimpled to 15 um and ion-milled by Ar gas. A JEOL 2000FX analytical electron microscope equipped with Kevex "Quantum"

energy-dispersive X-ray spectrometers (EDS) was used to characterize microstructure and composition. The EDS system has an ultrathin-window and can detect elements B though U.

SECTION 4

RESULTS AND DISCUSSION

4.1 Pressureless Densification

The sintered density of the alloys as a function of temperature, amount of sintering aid, various types of sintering aids, and SiC powders are discussed later in this section.

Figure 1 compares the density of the alloys which were prepared from different SiC powders and different sintering aids and fired at different sintering temperatures without using packing powders. It is quite clear that alloys prepared from Lonza alpha-SiC (AY2, AAY2 and AA2) have better density than those prepared from Starck alpha-SiC powder (BY2, BAY2 and BY2). The difference in density of these two groups of samples might be related to the sinterability of the SiC powder. Although the surface area of these two SiC powders were about the same, the agglomeration states of the powders may affect sinterability of SiC powders and overall density of the alloys.

Figure 1 also shows that the alloys using yttria as a sintering aid, either AY2 or AAY2, have higher density than alumina-doped samples, AAY2. Therefore, the results indicate that yttria is a better sintering aid than alumina. Moreover, the density curves also show that optimum sintering temperature was about 2050 to 2100°C. Higher sintering temperature did not yield better density. The maximum density in this set of samples under the

sintering conditions without using packing powder is only 2.83 gm/ml, which is about 88% T.D. and not high enough for real application.

More yttria sintering aid (4%) was put into alloys to increase the sintered density and the results are shown in the Figure 2. The alloys prepared from the mixture of Lonza alpha-SiC and Starck AlN (AY4) had better density than other two (SBY4 and BY4). Near 98.5% theoretical density can be achieved when AY4 is sintered at or higher than 2050°C. The results demonstrate that 4 wt% of yttria sintering aid is better than 2 wt% and high density can been achieved even under sintering conditions without using packing powders. Figure 2 also reveals that the density of SBY4 and BY4 decrease 10% as the sintering temperatures increase over than 2050°C. The surface of these samples was found to have a porous surface layer, especially at the corners of the sintered piece.

Figure 3 shows the densities of alloys with 4 wt% yttria after sintering at 2050°C for 1, 2 and 4 hours. The results indicate that 1 to 2 hr is an optimum sintering period. A longer sintering period did not improve the fired density.

All the data shown in Figures 1 to 3 are from the alloys sintered without using packing powders. Under this sintering condition, a degradation layer at the surface of the samples was observed. SEM and EDS were used to characterize the layers. Figure 4 shows the polished surface of SBY4 which was sintered at 2050°C for 4 hr. This degradation layer contains more pores than the center of the sample. The EDS results (Figure 5) showed the grains are much richer in Si element than the matrix. It implies that a loss of an Al-related phase might occur through the decomposition of AlN during sintering at 2050°C or higher. Moreover, a yttria-rich phase (bright contrast grains)

was also found to be more concentrated in this degradation layer. Therefore, an experiment was conducted to investigate the necessity of packing powder.

Table 4 summarizes the densities of seven alloys sintered in different packing powders, and compares them to the case without using packing powder. The alloys sintered with packing powder have better density than those without using packing powders. The packing powders effectively reduced the degradation and improved the densification. The packing powders were also found to reduce the yttria segregation at the surface, and only 2 wt% of yttria was required to yield high density of AY2. Table 4 also shows that alpha packing powders yielded better composite density than beta packing powders, but the reason is not yet clear. The mechanism for the formation of the degradation layer and the ways to avoid it need to be further studied. Moreover, Table 4 also demonstrates that yttria was a better sintering aid than alumina or calcia.

TABLE 4 DENSITY OF AlN-SiC ALLOYS AFTER SINTERING AT 2050°C FOR 2 HR WITH OR WITHOUT PACKING POWDERS

Sample	Density		
	No Packing	In beta-PP	In alpha-PP
AY4	3.15	3.15	3.20
BY4	2.63	2.76	3.08
SBY4	2.86	2.98	3.18
AY2	2.99	2.82	3.18
BY2	2.49	2.51	2,78
AAY2	2.61	2.60	2.89
BAY2	2.44	2.39	2.63
AA2	1.95	---	2.01
AC2	---	---	2.12

All the discussion above was for the alloys with one-to-one AlN/SiC ratio. The densities of different alloys with different AlN/SiC ratios after sintering in the alpha-packing powder at temperatures up to 2150°C are shown in Figure 6. To achieve sintered density higher than 98% T.D. different temperatures are required for the alloys with different AlN/SiC ratios. The alloys with high AlN can be densified as low as 1920°C; but for alloys containing high SiC, a higher temperature (2100°C) was required for full densification. All the alloys above can be sintered to high density at temperatures from 2050 to 2100°C by using 2 wt% yttria and packing powders.

4.2 Microstructure and Phase Characterization

4.2.1 X-ray diffraction analysis

a) Phase of as-sintered materials

As discussed in the last section, the optimum sintering temperature of SiC-AlN alloys was about 2050-2100°C. The specimens sintered in this temperature range without using packing powder had a surface degradation layer, which was rich in yttrium and silicon (Figures 4 and 5). The X-ray diffractometry analysis on the as-fired surface and ground surface are shown in Table 5. The major phase in the as-fired surface was 6H and the minor phases were 2H and 15R. After the degradation layer was polished away, the ground surface showed a major 2H phase and minor 6H and 15R phases. When packing powders were used, the degradation layer could be reduced and the as-fired surface had similar phases at the center of the specimens. The (002) peaks in the X-ray diffraction patterns of Figure 7 also revealed that the as-fired surface of the alloys sintered without using packing powder had more SiC phase and stronger 6H peak, indicating that AlN might decompose

and evaporate from the surface at high temperature. The packing powder could reduce this decomposition reaction, then the surface would have similar phases as existed inside. Therefore, the sintered density was higher when the specimens were fired with packing powder.

b) Solid solution heat treatment and lattice parameter

The other important information from Figure 7 was the splitting (002) peaks, indicating that the SiC-AlN alloys at 2050°C were still in the two phase region and confirmed the miscibility gap below 2100°C as suggested by Ranfaniello et al.[4] In order to get a homogeneous solid solution, the specimens were heat treated at higher temperature after achieving full density at 2050°C. The solid solution temperature was first tried at 2100°C, but the X-ray diffraction patterns still showed multi-phases. Then the solid solution temperature was increased to 2200°C for a period of one hour. The X-ray diffraction patterns of four different SiC-AlN alloys after this heat

TABLE 5 PHASE OF AlN-SiC ALLOYS AFTER SINTERING AT 2050°C WITH OR WITHOUT PACKING POWDERS

Sample	Firing Condition	Phases	
		As-fired surface	Ground surface
AY4	2050°C 2h No packing powder	Major: 6H Minor: 2H, 15R	Major: 2H (split) Minor: 6H, 15R
	2050°C 2h alpha packing powder	Major: 2H (split) Minor: 6H, 15R	Major: 2H (Split) Minor: 6H,15R

treatment condition are shown in Figure 8. For the specimens rich in AlN (7/3Y2), only 2H peaks were found, indicating a possible single solid solution phase. However, these peaks were broader than normal peaks and the deconvolution analysis showed that there were two peaks under one broader peak. For the composition with a one-to-one ratio of AlN and SiC (AY2 and SBY4), the alloys prepared from beta SiC powder (SBY4) had broader 2H peaks, and deconvolution analysis also identified the multi-phase. The alloys prepared from alpha SiC powder (AY2) had major split 2H peaks and minor 6H and 15R phases. For the alloys rich in SiC (3/7Y2), the 4H were found to be the major phase, and minor phases were 2H, 6H and 15R. The two peaks resulting from the single broadened peak by using deconvolution were closer to each other than those of pure AlN and SiC, indicating that AlN and SiC had already formed some solid solution: one is rich in SiC and the other was rich in AlN, but the single solid solution phase had not been achieved. None of the alloys above showed single phase. So a single homogeneous solid solution phase had not been achieved up to 2200°C. The result is quite different from the work done by Ruh and Zangvil[3], where they showed that solid solution of the hexagonal 2H structure could form at the temperature above 2100°C when the alloys contained 35 to 100% AlN.

The solid solution temperature was then further increased to 2225°C for 3 hrs. The X-ray diffraction patterns of the samples after sintering and solid solution treatment are shown in Figure 9. Three of the four alloys had achieved single solid solution 2H phase and only the specimen with high SiC content (3/7 Y2) did not achieve single solid solution 2H phase; minor 6H, 4H and 15R also were found. Both beta and alpha SiC powder could be used to prepare single solid solution SiC and AlN (AY2 and SBY4). No

difference was observed from using different types of SiC powder; this is different from the observation of Kuo et al[10]. These results also demonstrated that the specimens with high AlN content could form single solid solution easier, which is similar to the result of Ruh and Zangvil.[3] However, the solid solution temperature did not fit the tentative SiC-AlN diagram as suggested by them,[16] where the critical temperature to achieve the solid solution phase was 1900°C. This tentative phase diagram included the data by Rafaniello et al.[2], in which the SiC-AlN powder was prepared by carbon thermal reduction; larger surface area and intimate mixture were believed to facilitate the formation of the solid solution. However, the AlN-SiC powder prepared by carbon thermal reduction by same authors[4] showed nonhomogeneous phases when hot-pressed at or below 2100°C. Ruh and Zangvil[3,8] also found 4H and 15R phases accompanying the 2H phase after hot pressing the mixture of SiC and AlN powders at 2100°C. But Tsukuma et al[5] had demonstrated that solid solution could be achieved at 1800°C through the reaction of Si_3N_4 and Al_4C_3 at high pressure. That might be related to the effects from the impure raw materials and the pressure and/or atmosphere as had been noticed by Zangvil and Ruh[16]. Despite the difference in the temperature for forming single 2H solid solution as discussed above, the temperature should be higher than 2100°C when using commercially available pure SiC and AlN powders. Of course, the discrepancy in the solid solution temperature might be due to kinetics, instead of thermodynamics. The slow diffusion rate of AlN and SiC made it more difficult for the alloys to achieve equilibrium composition.

The alloy rich in SiC (3/7Y2) finally was brought to single solid solution after the solid solution temperature was increased to 2300°C. The

precise lattice parameter of SiC-AlN solid solutions containing different AlN/SiC ratio are summarized in Table 6 and plotted in Figure 10. The a-lattice of SiC-AlN decreased as SiC content increased. At the same time, the c-lattice increased. The extrapolation of the lattice parameter of solid solution fitted both pure AlN and SiC lattice parameters reasonably well.

c) Phases of the annealed samples

The SiC-AlN alloys having single 2H solid solution phase were than annealed at 1860°C for 24, 48 and 96 hrs for precipitation study. There was very little change in the x-ray diffraction patterns of 73Y2, AY2 and SBY4 until they were annealed to 96 hrs. Figure 11 compares the diffraction patterns of the alloys before and after 96 hr of annealing. The split 100 and 002 peaks indicated the decomposition of the 2H solution after long annealing, and confirmed the possible miscibility gap suggested by Rafaniello et al[4]. The long annealing time required to decompose the solid solution also reflected the low diffusion rate of SiC and AlN. The microstructure of these samples is discussed later.

TABLE 6 LATTICE CONSTANTS OF SiC-AlN ALLOYS

Materials AlN (%)	Materials SiC (%)	a-lattice (A)	c-lattice (A)	note
100	0	3.11100 (6)	4.9797 (4)	before sintering
100	0	3.11152 (16)	4.9776 (6)	after sintering
70	30	3.10606 (5)	5.0064 (3)	
50	50	3.09813 (13)	5.0223 (9)	beta SiC
50	50	3.09854 (17)	5.0213 (8)	alpha SiC
30	70	3.09050 (8)	5.0374 (5)	
0	100	3.0763	5.048	PDF 19-1138
0	100	3.081	5.031	PDF 29-1126

4.2.2 Optical microscopy

The optical microstructure of the polished and then etched sample is shown in Figure 12. The microstructure demonstrated that the SiC-AlN is highly dense and homogeneous. The grain size was about 3 to 5 um.

4.2.3 Transmission electron microscopy (TEM)

a) As-sintered

The X-ray diffraction patterns showed multi-phase even after the materials were heated up to 2100°C as discussed in the Section 4.2.1. Under the TEM at high magnification, the microstructure was found to be composed of large AlN-rich grains, small SiC-rich grains and a yttria-rich grain boundary phase as shown in the Figure 13. The EDS results of Figure 13 show that large AlN grains contain a certain amount of SiC, but small SiC grains did not contain much of AlN, indicating that the SiC diffusion rate in the AlN was faster than that of AlN in the SiC grains. Most of the grain boundary phase was concentrated at the triple junction of grains, especially in the region of SiC cluster (see Figure 14) and contained Y, Al, Si, O, C, and N.

b) Solid solution treatment

Most of the as-sintered materials could be solid solution treated at 2225°C to achieve a single solid solution phase as discussed in the Section 5.2.1. The TEM microstructure of AY2 (see Figure 15) shows a homogeneous microstructure after solid solution treatment, but no SiC cluster grains were observed, confirming the XRD single solid solution results. The EDS analysis across one of the grains showed very homogeneous Si/Al ratio from edge to center of the grain (See Figure 16). In some grains, small SiC particles were found in the SiAlCN grain (See Figure 17). This feature was

believed to be related in that the small SiC particle was "eaten" by the SiAlCN grain during its grain growth, indicating that grain growth of SiAlCN was faster than the diffusion rate of SiC in the AlN. EDS results showed that the SiC particle only contained a small amount of Al, while the matrix grain contained an almost equal amount of SiC and AlN. So the diffusion rate of AlN in the SiC was quite slow. The trapped SiC particles, which did not completely dissolve in the SiAlCN grain, also indicate that the grain boundary diffusion, other than lattice diffusion, might play an important role for the formation of the solid solution.

The grain boundary phase in the specimens after solid solution treatment was different from the as-sintered material. Four different types of glass phase were found in different locations of the grains. One is at the triple junction and boundaries of grains (Marked A and B in Figure 18), containing relatively high Al and Si content. The second type is also located at the junction of the grains, but more grain boundary phase was accumulated together (marked C in Figure 18) and much less Si content was found. The phase might have yttrium-aluminum-garnet (YAG) structure with slight silicon dissolution. The third kind of grain boundary phase was trapped inside the SiAlCN grains (marked D in the Figure 18), sometimes with the hole at the center of this phase. This type of feature resulted from the trapping of the glassy phase during the grain growth of SiAlCN at high temperature. The glassy phase then crystallized at lower temperature and the volume change during the crystallization caused formation of the pore at center of this phase. The round shape of this phase in the SiAlCN grains also indicated that the interface energy between them was quite large. The EDS results also showed that this phase was rich in Al and Y, but had not much Si content. The

last kind of grain boundary phase found in this specimen was quite different from the above three. The phase was rich in Si and Y and only a small trace of Al was found (see Figure 18(b)). The region of this phase was quite large (up to 10 um) and normally had a rectangular shape. These yttrium-rich phases are all crystalline according to their diffraction patterns, which is good for the mechanical properties of these alloys. The EDS results of the grain boundary phases are shown in Figure 19.

Two other compositions, 7/3Y2 and 3/7Y2, had similar microstructures after solid solution treatment, but the Al/Si ratios were quite different because of the composition, as shown in Figure 20.

c) Annealing treatment

After solid solution heat treatment, several specimens were annealed at 1860°C for the study of precipitation. Alloys with different AlN/SiC ratios had different microstructure after annealing; however, they all contained cleaner grain boundaries and most of the Y-rich phase was trapped in the SiAlCN grains instead of at grain boundaries (see Figure 21). The alloys containing a one-to-one ratio of AlN and SiC (55AY2 and SBY4) after annealing at 1860°C for 96 hr had unique and important microstructures, composed of equiaxed grains and elongated grains (Figure 22). Several different grains were analyzed for structure and chemical composition by using TEM and EDS. The equiaxed grains were found to have 2H structure and contain high AlN content. At higher magnification, the large 2H grains were found to have precipitates with modulate feature as marked A,B and C grains in Figure 23. The satellite peaks and streaking corresponding to the modulate structure can also be observed in the electron diffraction patterns. The

structure can also be observed in the electron diffraction patterns. The modulate feature spacing is about 50 nm, which is much larger than the modulate structure observed by Kuo and Virkar[14]. Moreover, the elongated grains accompanying the modulated feature had not been observed by them. The mechanism for forming modulate structure was proposed to be spinodal decomposition.[14] The elongated grain marked D in the Figure 23 was confirmed to be faulted 3C structure by taking diffraction pattern at [110] zone. The streaking in the diffraction pattern also indicated that it contained heavily faulted structure and possibly some other polytype. EDS results of the elongated grains and the grains around it are shown in Figure 24. It is quite clear that the elongated grain with 3C faulted structure was much richer in SiC than other equiaxed grains. Only about 7% AlN was contained in this 3C phase, while the center of the large equiaxed grains contained more than 45% of AlN. It was also noticed that the elongated grain was not exactly rectangular in shape. The concave area (marked C) was part of the grain B and had more AlN content than the elongated grain, but much less than the rest of the grain B. Several diffractions were taken at the grains around the elongated grains and no apparent crystallographic relationship between them were observed.

Some other areas were also analyzed. It was found that the equiaxed grains always had 2H structure with modulate feature, and the elongated grains can have different structures, such as 6H (see Figure 25) and other polytype with heavy faulting (see Figure 26). EDS analysis again showed that lower content (10%) of AlN was found in the elongated grains and higher AlN content in the equiaxed grains. These results indicate that the formation of elongated grains has a close relationship to the redistribution

of AlN and SiC during annealing. Further research is required to fully understand the mechanism.

The microstructures of the alloys with high AlN content (73Y2) and high SiC content (37Y2) are quite different. Most of the grains in the 73Y2 were equiaxed 2H grains with modulate structure. On the other hand, the 37Y2 alloys had a lot of elongated grains, as shown in the Figure 27. It is quite clear that the ratio between elongated grains and equiaxed grains with modulated feature can be controlled by the AlN-to-SIC ratio.

4.3 Preliminary mechanical properties

The unique duplex structure which is composed of elongated and equiaxed grains is very important. The elongated grains can increase toughness of the alloys by a crack-deflection toughening mechanism[17]. One example of the crack deflection due to the elongated grains is shown in the Figure 28. The crack results from the 20 kg load indent. Figure 29 compares the indents on pure SiC, pure AlN and annealed 37Y2 materials. From the size of the indent, it is quite clear that the alloy is much harder than AlN and close to the hardness of SiC. The fracture toughness can be estimated from the indent size and crack length according to the equation developed by Nihara et al.[18] The SiC had toughness about 3 $MPam^{1/2}$ and the AlN had toughness bout 3.4 $Mpam^{1/2}$. However, the 37Y2 had fracture toughness about 6 $MPam^{1/2}$, which is twice that of pure SiC. Moreover, the creep resistance is also expected to be increased because of the elongated grains if the grain boundary sliding is the dominant mechanism for high temperature creep. On the other hand, if the creep is dominated by the dislocation climb, the modulate structure in the equiaxed grains should increase creep resistance by retarding

the movement of dislocations. Therefore, this alloy can have good toughness at room temperature and good creep rupture resistance at high temperature. Further work is required to fully explore this material.

SECTION 5

CONCLUSIONS AND FUTURE WORK

The objectives proposed in Phase I of this research project have been successfully achieved. The important discoveries are summarized below.

1) Highly dense SiC-AlN alloys with unique microstructure and fracture toughness up to 6 $MPam^{1/2}$ were successfully produced. The sintering aids required for pressureless sintering and the process for preparing the alloys were identified. The alloys can have desirable microstructure and properties after optimum heat treatment.

2) The SiC-AlN alloys can be prepared from commercial SiC and AlN powders with the addition of yttria as a sintering aid, a method easier and less expensive than other processes. Both alpha and beta SiC powders can be used to prepare the alloy, although the alloys prepared from alpha SiC have better density at lower temperatures. The green body of the alloys can be prepared by conventional ceramic processing, such as slip casting, pressure casting and dry pressing, and then be pressureless sintered to high density.

3) The SiC-AlN alloys can be pressureless sintered to full density by using yttria as a sintering aid. The yttria sintering aid is better than alumina and calcia and only 2 wt% yttria was required to get high density. The mechanism for densification is proposed to be liquid phase sintering.

4) Different alloys have different optimum temperatures for achieving high density. The alloy with higher AlN content can be densified at lower temperatures, but all of the alloys can achieve high density at 2050 to 2100°C. An inert gas, such as argon, and N_2 can be used during sintering. Packing powders can be used to protect the specimens and prevent degradation during firing.

5) The sintered SiC-AlN alloys can achieve single solid solution after solution treatment at temperatures higher than 2225°C. The lattice constant of the solid solution varied linearly as the SiC/AlN ratio changed.

6) The AlN-SiC alloys after solid solution had equiaxed grains with 2H structure. Most of the yttrium-rich phase which assisted densification during liquid phase sintering were trapped inside the grains and leave clean grain boundaries. The yttrium-rich phases were all crystallized, which should give reasonable mechanical properties.

7) Annealing at 1860°C yielded a unique and important microstructure, composed of equiaxed grains with modulate feature, elongated grains with heavy faulting and clean grain boundaries. The equiaxed grains have a 2H structure and contained more AlN than the elongated grains. Normally, the elongated grains contained less than 10% AlN and had a lot of different polytypes. The ratio of equiaxed grains and elongated grains can be controlled by the ratio of AlN and SiC.

8) The alloys are expected to have good mechanical properties based on the unique duplex microstructure. The preliminary mechanical results showed that the alloys can have fracture toughness up to 6 $Mpam^{1/2}$, about twice that of pure SiC and comparable to monolithic or whisker reinforced Si_3N_4. The increase in fracture toughness was due to the crack deflection of the elongated grains.

In summary, highly dense SiC-AlN alloys were successfully produced by pressureless sintering. After appropriate annealing, the alloys have an exceptional microstructure. The microstructure was composed of equiaxed grains with modulate feature, elongated grains with heavy faulting and clean grain boundaries. The fracture resistance and high temperature creep resistance of these alloys are believed to be good based on this unique microstructure. Preliminary results already show that the toughness is increased to 6 $Mpam^{1/2}$. More research is required to bring these alloys into real application. The detailed research plan is discussed in the Phase II proposal. Following are the key points suggested for future research:

1) Scale up the production of these alloys and test mechanical properties statistically. The chevron notch testing technique will be used to measure fracture toughness, and the four point bend test will be used to measure flexure strength. High temperature flexure strength and creep resistance will also be evaluated to see whether these alloys can be used for high temperature application.

2) Define a process to achieve high fracture toughness and strength through more studies on the correlations between microstructure, processing and properties. Current results already demonstrate that the microstructure of these alloys can be controlled by alloying, sintering and heat treatment. More research is required to fully characterize and correlate them with mechanical properties.

3) Identify the alloys exhibiting better mechanical properties. Our results have shown that the ratio of elongated grains to equiaxed grains can be controlled by the SiC/AlN ratio. Through the research on the correlation between the mechanical properties and microstructure of different alloys, better ceramic alloys can be designed.

4) Identify the process to produce complex geometric parts, such as a turbine rotor. The alloys have been successfully produced by pressureless sintering, which is a better and less expensive way for fabricating complex parts. Evaluation of the process for green part preparation and sintering conditions needed to produce complex parts with good properties.

REFERENCES

1. I.B. Cutler, P.D.Miller, W. Rafaniello, H.K. Park, D.P. Thompson, and K.H. Jack, "Mew Materials in the Si-C-Al-O-N and Related Systems", Nature, V 275, 434, 1978

2. W. Rafaniello, K. Cho and A.V. Virkar, "Fabrication and Characterization of SiC-AlN Alloys", J. Mat. Sci. V 16, p3479-3488, 1981

3. R. Ruh, and A. Zangvil, "Composition and Properties of Hot-Pressed SiC-AlN Solid Solutions", J. Am. Ceram. Soc., 65, p260-265, 1982

4. W. Ranfaniello, M.R. Plichta, and A.V. Virkar, "Investigation of Phase Stability on the System SiC-AlN", J. Am. Ceram. Soc., 66, 272-276, 1983

5. K.Tsukuma, M. Shimada, M. Koizumi " A New Compound Si3Al4N4 C3 with the Wurtzite Structure in the System Si3N4-Al4C3", J. Mat. Sci. Let., 1, (1982), p9

6. M. Shimada, K Sasaki, and M. Koizumi, "Fabrication and Characterization of ALN-SiC Ceramics by High Pressure Hot-Pressing", p466-472 in "Processing of International Symposium on Ceramic components for Engine", 1983

7. A. Zangvil and R. Ruh, "The Si3Al4N4C3 and Si3Al5N5C3 compounds as SiC-AlN Solid Solution", J. Mat. Sci. Let., 3, (1984), 249-250

8. A. Zangvil and R. Ruh, "Solid Solution and Compositions in the SiC-AlN and SiC-BN Systems", Material Sci. and Eng., 71, (1985) p159-164

9. R.Ruh, A. Zangvil, and J. Barlowe, "Elastic Properties of SiC, AlN, and their Solid Solutions and Particulate composites", Am. Ceram. Soc. Bull., 64, p1368-1373, 1985

10. S.Y. Kuo, Z.C. Jou, and A.V. Virkar, and W. Rafaniello, "Fabrication, Thermal Treatment and Microstructure Development in SiC-AlN-Al_2OC Ceramics", J. Mat. Sci., 21, p3019-3024, 1986

11. Z.C. Jou, S.Y. Kuo, and A.V. Virkar, "High Temperature Creep in Polycrystalline AlN-SiC Ceramics", J. Mat. Sci., 21, 3015-3018, 1986

12. Z.C. Jou, S.Y. Kuo, and A.V. Virkar, "Elevated-Temperature Creep of Silicon Carbide-Alumina Nitride Ceramics: Role of Grain Size", J. Am. Ceram. Soc., 69, C-279 to C-281, 1986

13.J.-L. Huang, A.C. Hurford, R.A. Cutler and A.N. Virkar, "Sintering Behavior and Properties of SICALON Ceramic", J. Mat. Sci., 21, 1448-1456, 1986

14. S. Y. Kuo and A.V. Virkar, "Modulated Structures on SiC-AlN Ceramics", J. Am. Ceram. Soc., 70 [6], C-125- C-128, 1987

15. W.T. Donlon, J. Hangas, C.R. Peters, S. Shinozaki, and K. Maeda, "Microstructural Analysis of Hot-Pressed SiC-AlN", #21-BP-88, presented in Am. Ceram. Soc. Annual Meeting 1988

16. A. Zangvil and R. Ruh, "Phase Relationships in the Silicon Carbide-Aluminum Nitride System", J. Am. Ceram. Soc., 71, p884-890, 1988

17. K.T. Faber and A.G. Evans, Acta Metall. 3, 565,1983

18. K. Niihara, R. Morena and D.P.H. Hasselmann, "Evaluation of K_{Ic} of brittle solids by indentation method with low crack-to indent ratios, J. Mat. Sci. Lett. 13-16, 1982.

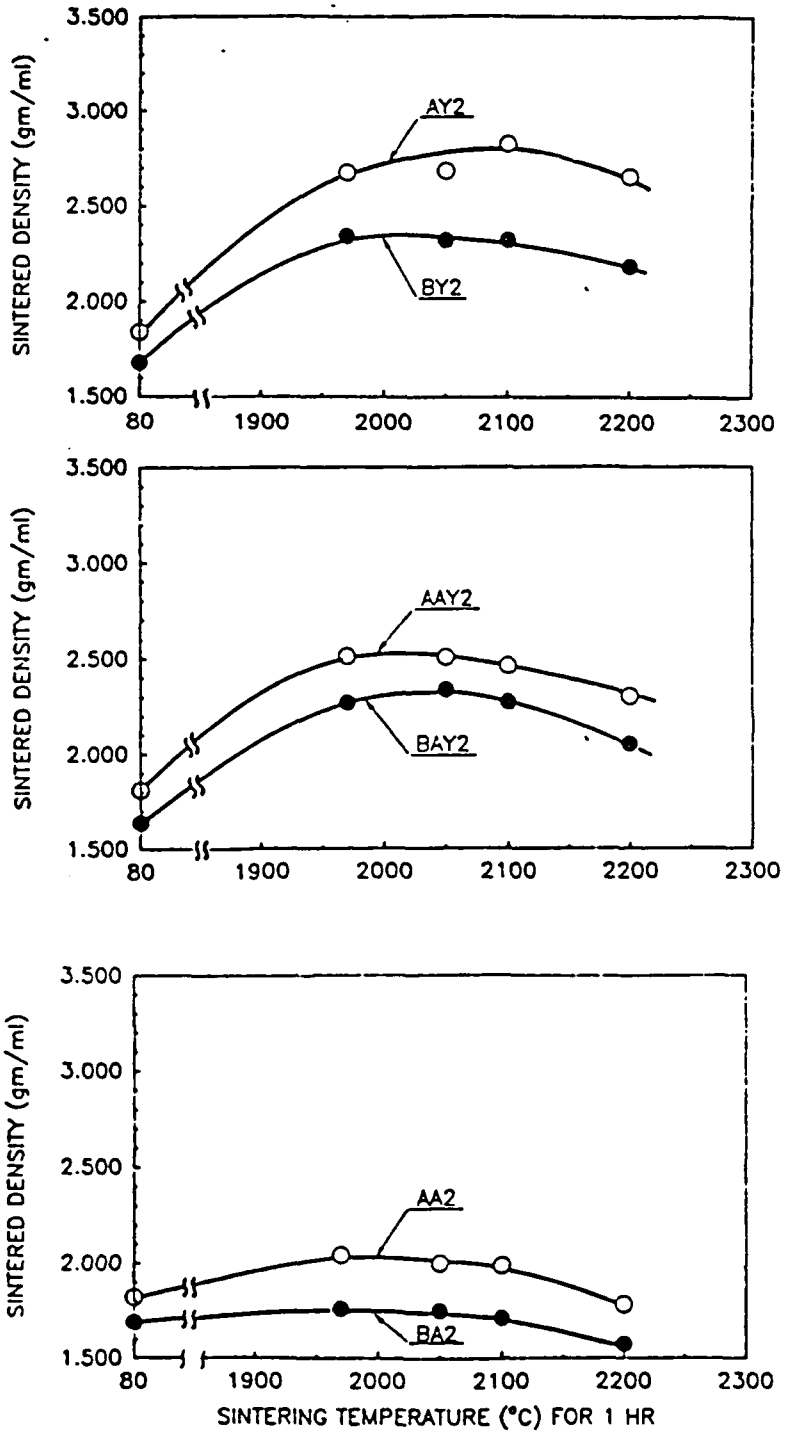

Figure 1 Density of AlN-SiC alloys after sintering at 1960 to 2200°C in Ar atmosphere without burying in packing powder. (a) 2 wt% yttria sintering aid, (b) 1 wt% yttria and 1 wt% alumina (c) 2 wt% alumina

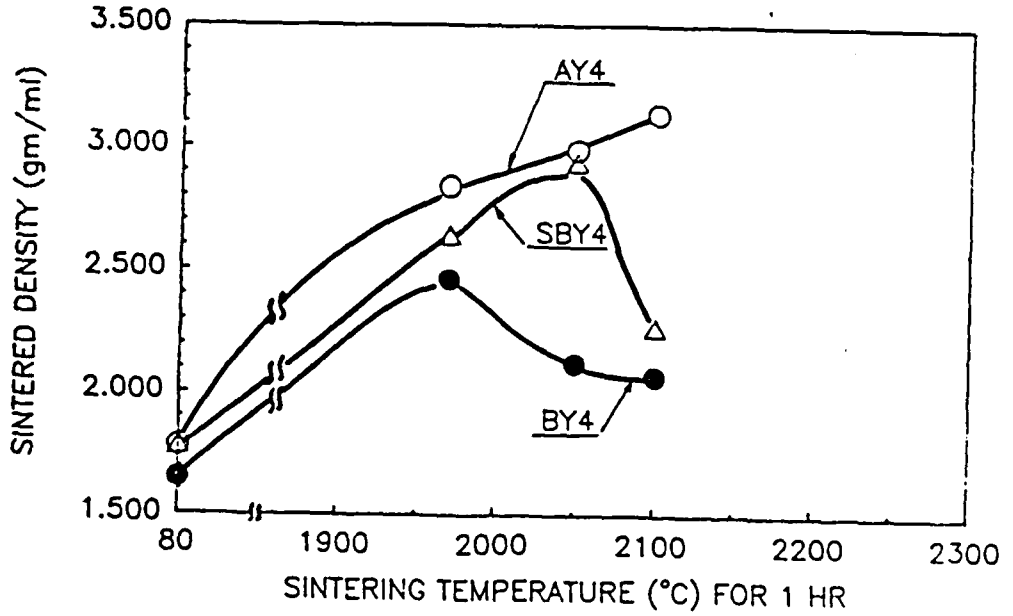

Figure 2 Density of AlN-SiC alloys with 4 wt% yttria sintering aid at different temperatures without using packing powders

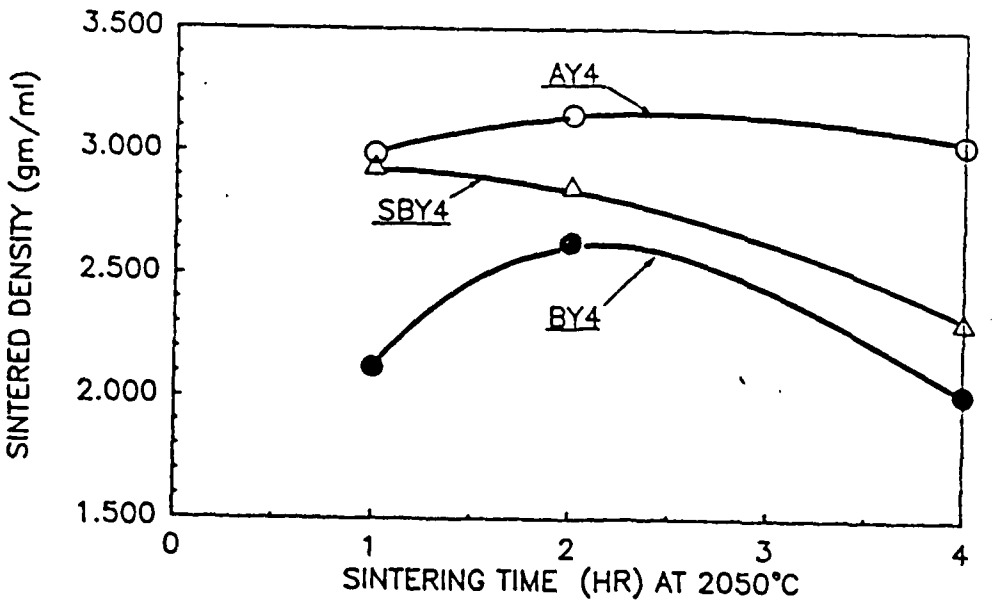

Figure 3 Density of alloys with 4 wt% sintering aid at 2050°C for various times

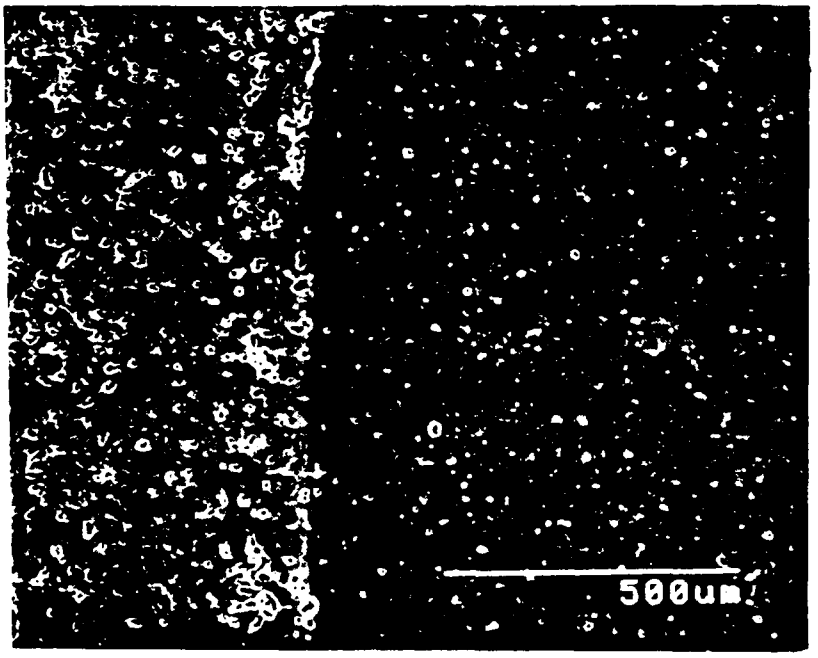

(a)

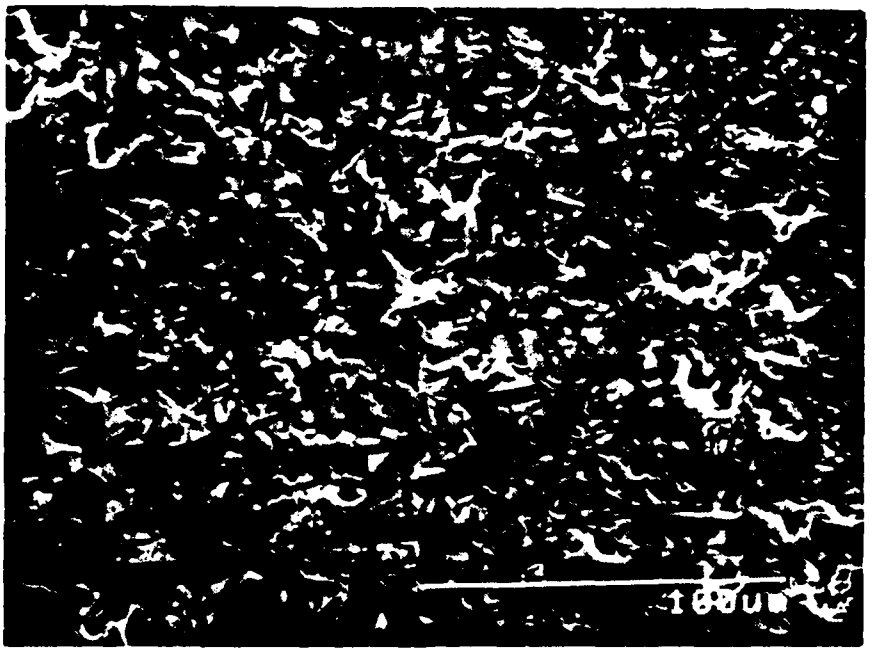

(b)

Figure 4 SEM micrograph showing surface degradation of sample AY4 (a) after sintering at 2050°C for 4 hr without using packing powder, (b) higher magnification at the surface layer

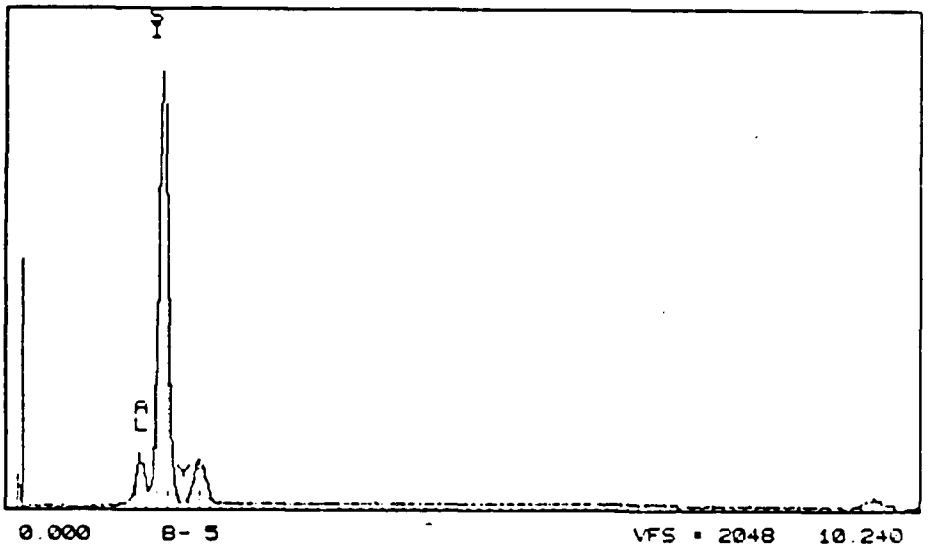

(a)

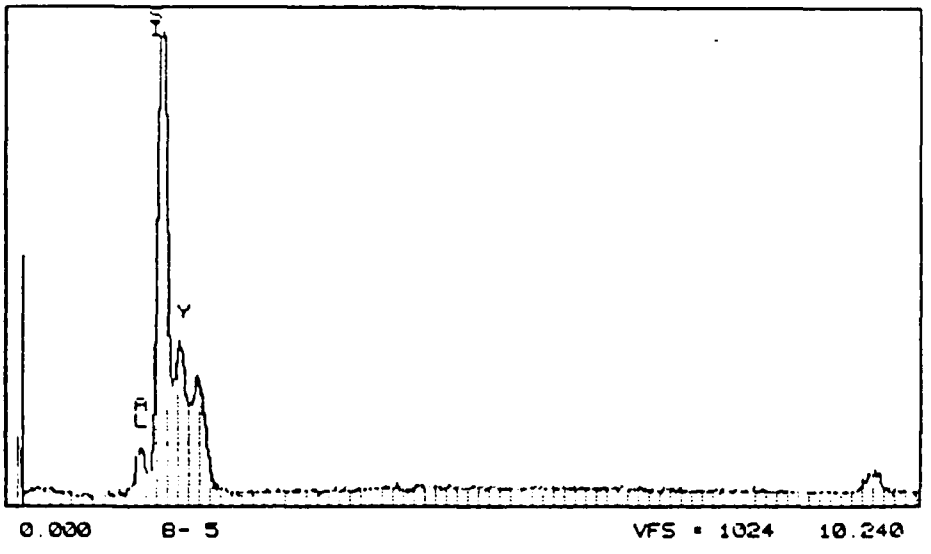

(b)

Figure 5 EDS spectra of the dark and bright regions in Figure 4(b), (a) dark area, (b) bright area

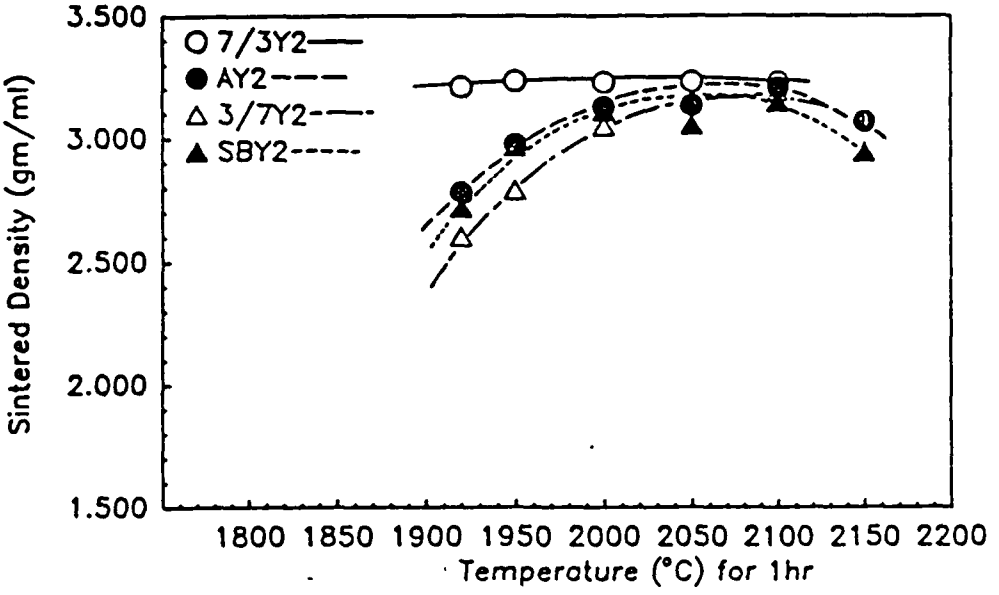

Figure 6 Density of alloys after sintering at different temperatures with samples buried in packing powder

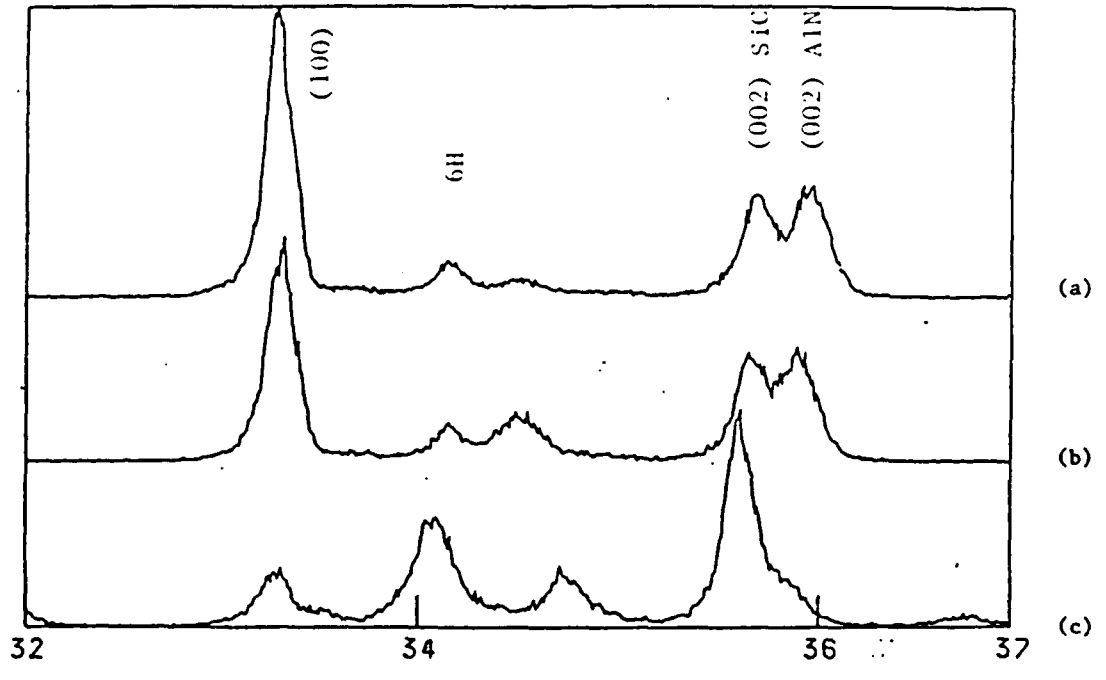

Figure 7 XRD patterns of the as-fired surfaces of AY4 (a) in beta-SiC and AlN packing powders, (b) in alpha-SiC and AlN packing powders, (c) no packing powder

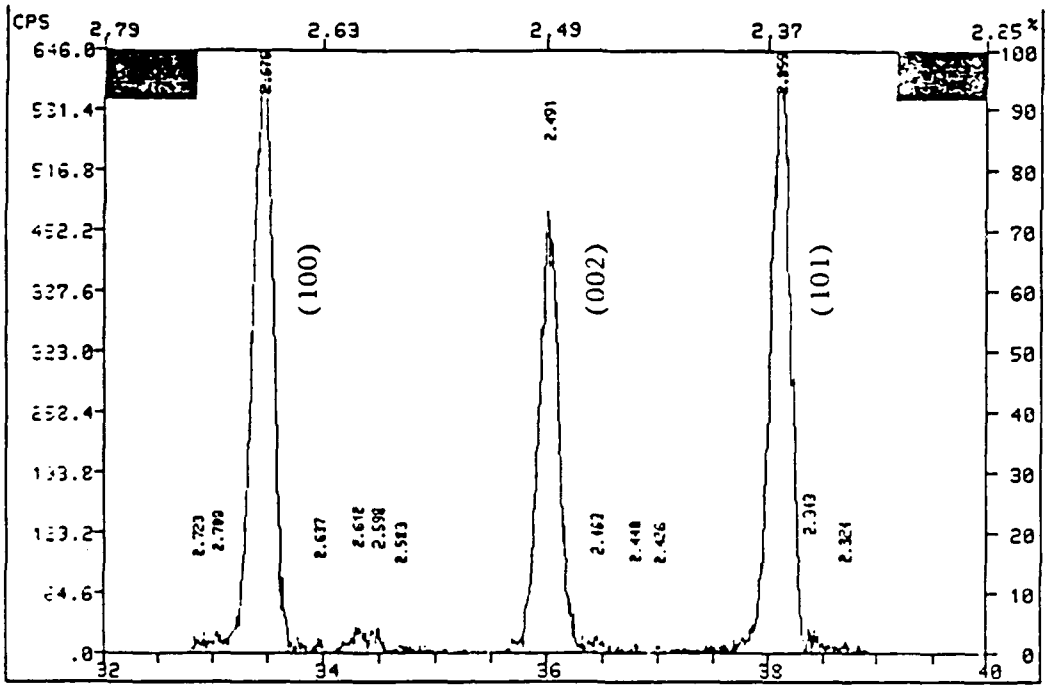

(a)

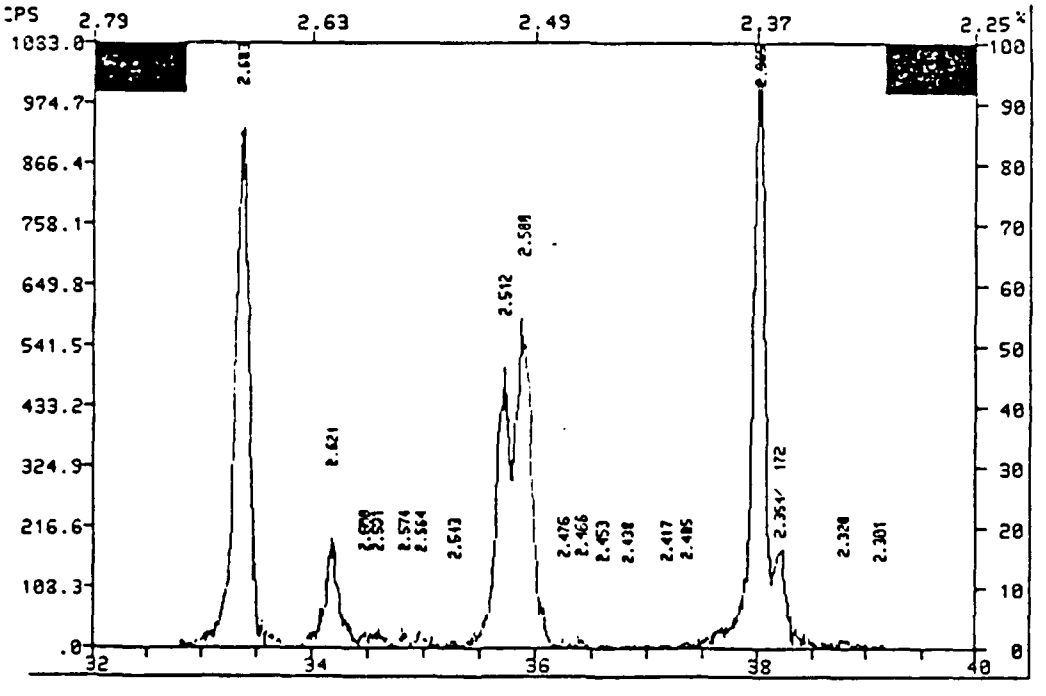

(b)

Figure 8 XRD patterns of SiC-AlN alloys after solid solution treatment at 2200°C for one hour (a) 73Y2, (b) AY2

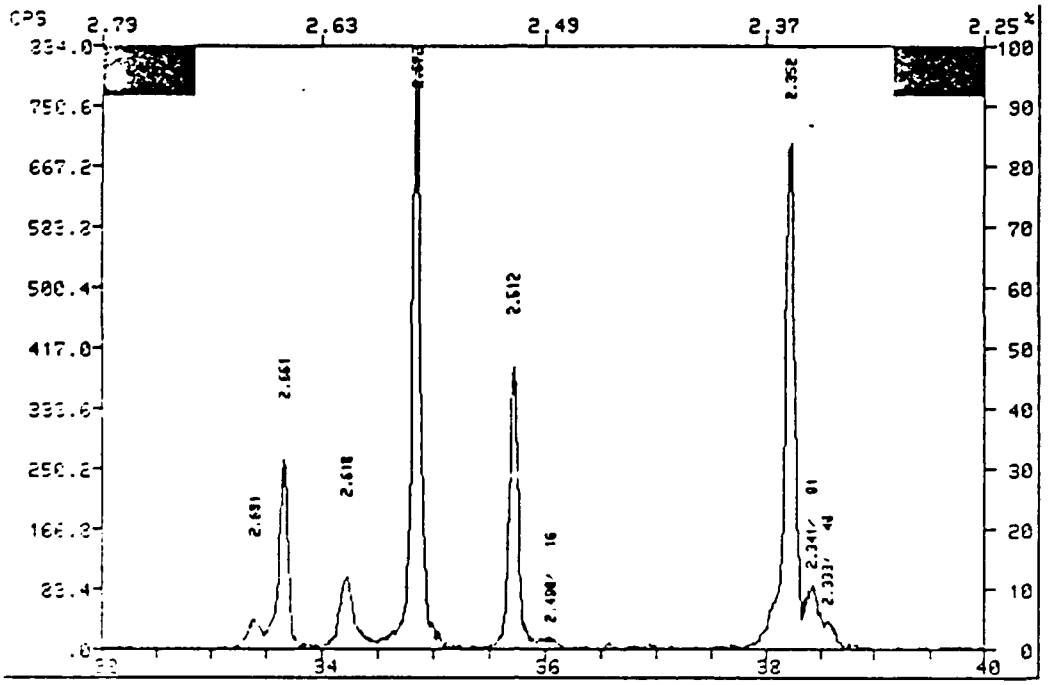

(c)

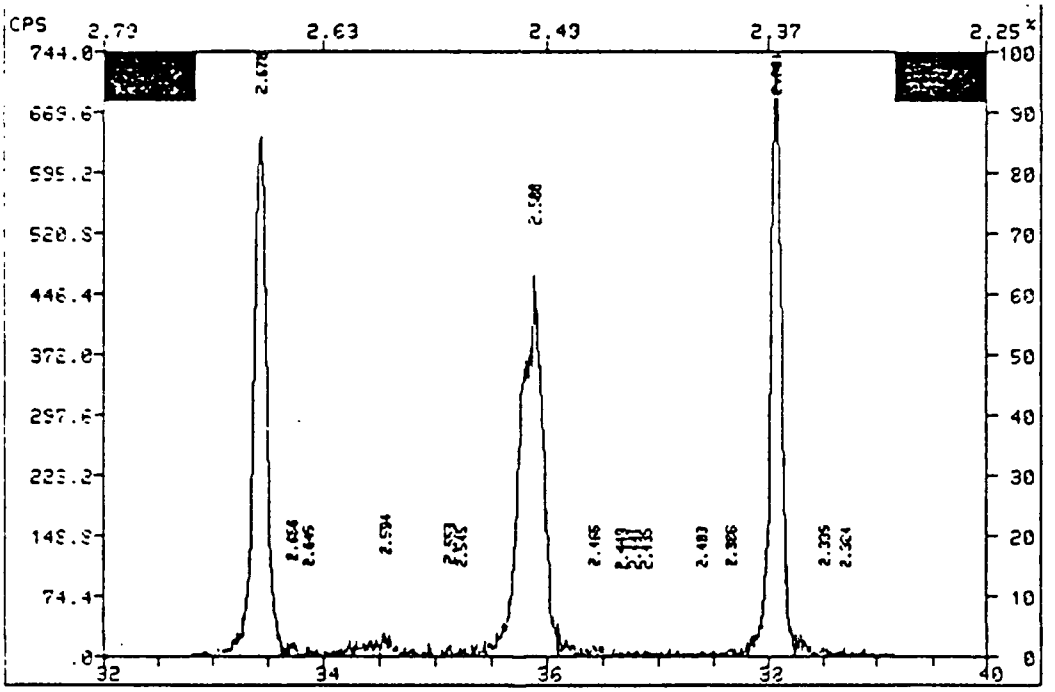

(d)

Figure 8 XRD patterns of SiC-AlN alloys after solid solution treatment at 2200°C for one hour (c) 37Y2, (d) SBY4

PK#	2-THETA	PK-TOP	FWHM
1	33.4976	27542.	.135
2	33.4048	225 0.	.151

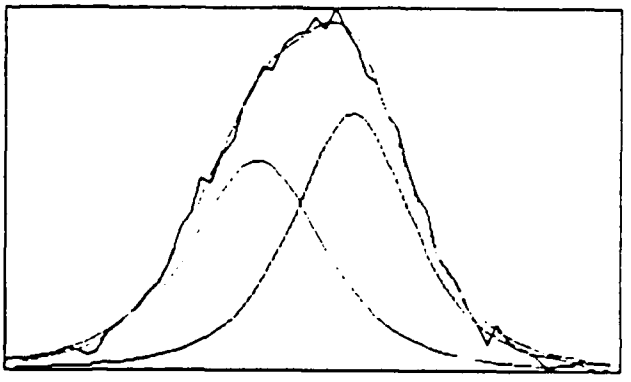

(e)

PK#	2-THETA	PK-TOP	FWHM
1	35.5062	23497.	.149
2	[illegible]	[illegible]	.125

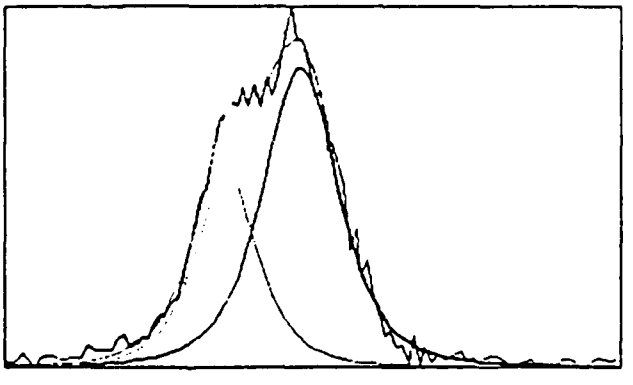

(f)

Figure 8 XRD patterns of SiC-AlN alloys after solid solution treatment at 2200°C for one hour (e) deconvolution of (100) peak of 73Y2 (f) deconvolution of (001) peak of SBY4

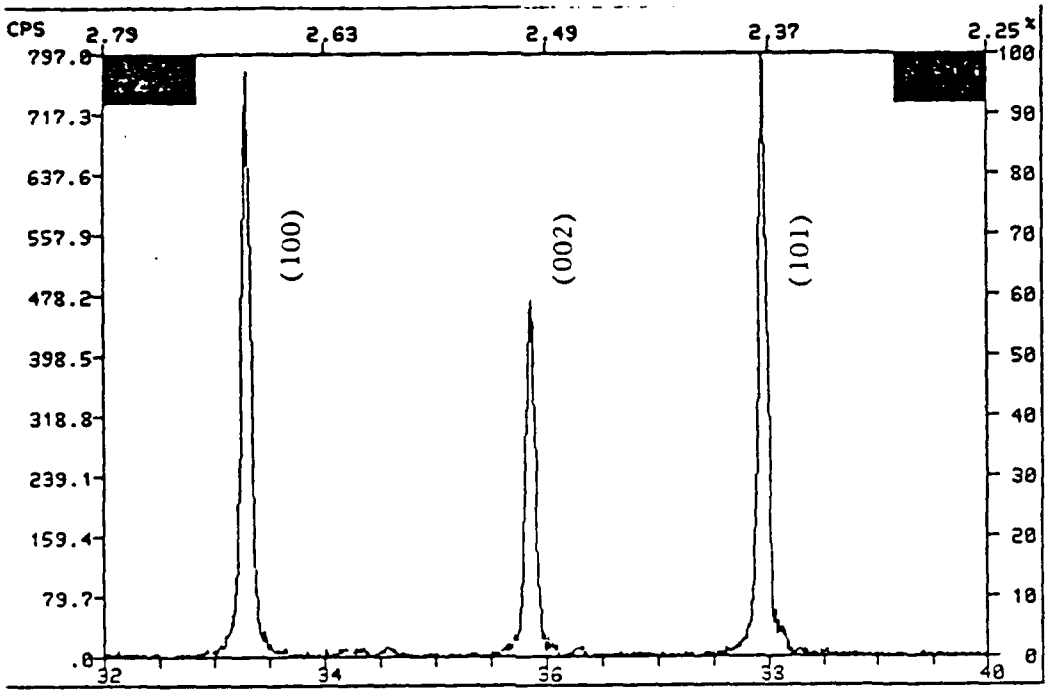

(a)

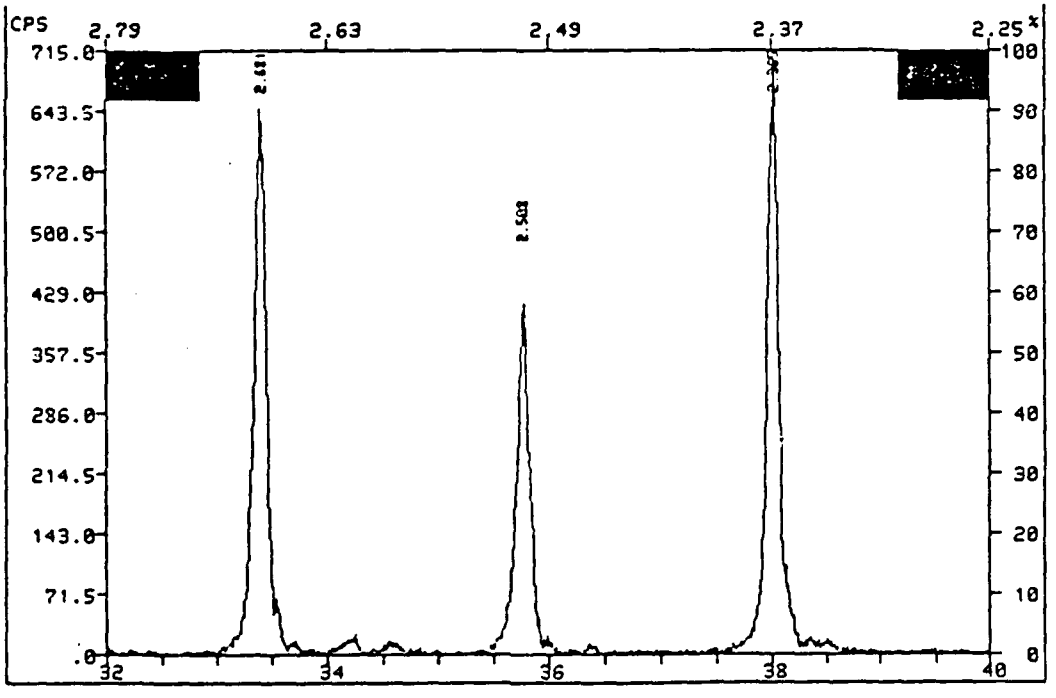

(b)

Figure 9 XRD patterns of AlN-SiC alloys after solid solution treatment at 2225°C for 3 hours (a) 73Y2, (b) AY2

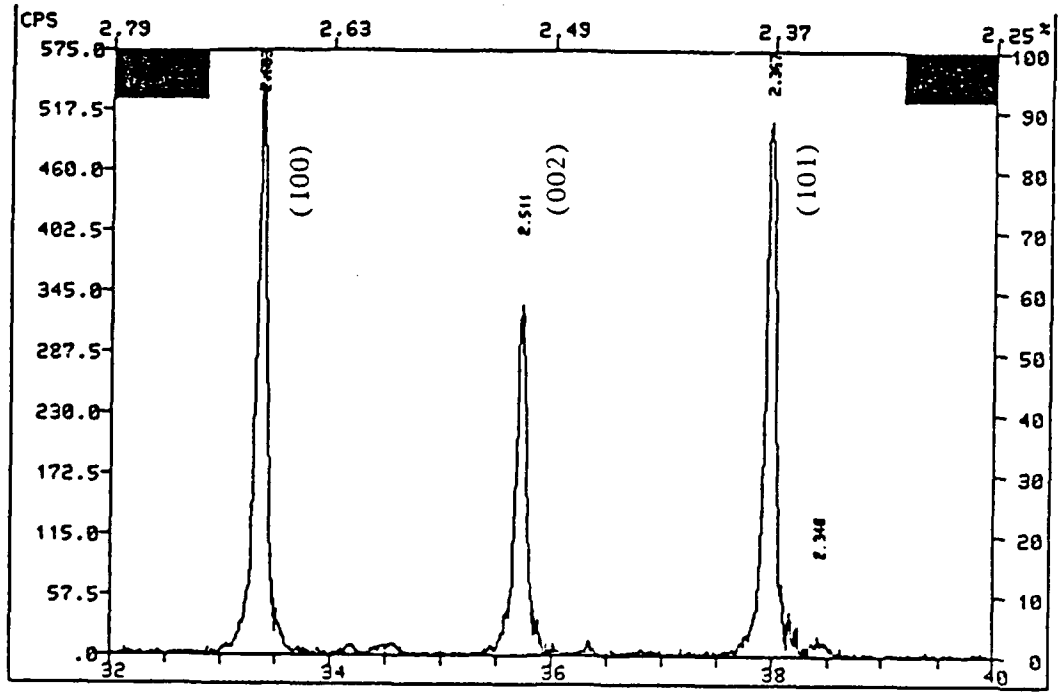

(c)

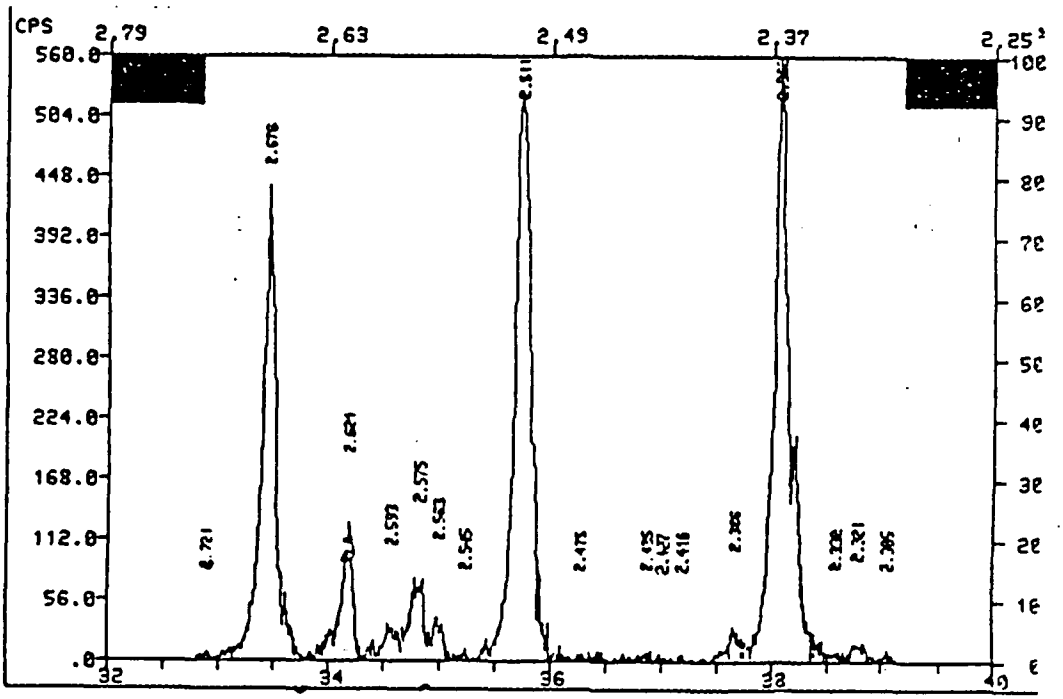

(d)

Figure 9 XRD patterns of AlN-SiC alloys after solid solution treatment at 2225(o) for 3 hours (c) SBY4, (d) 37Y2

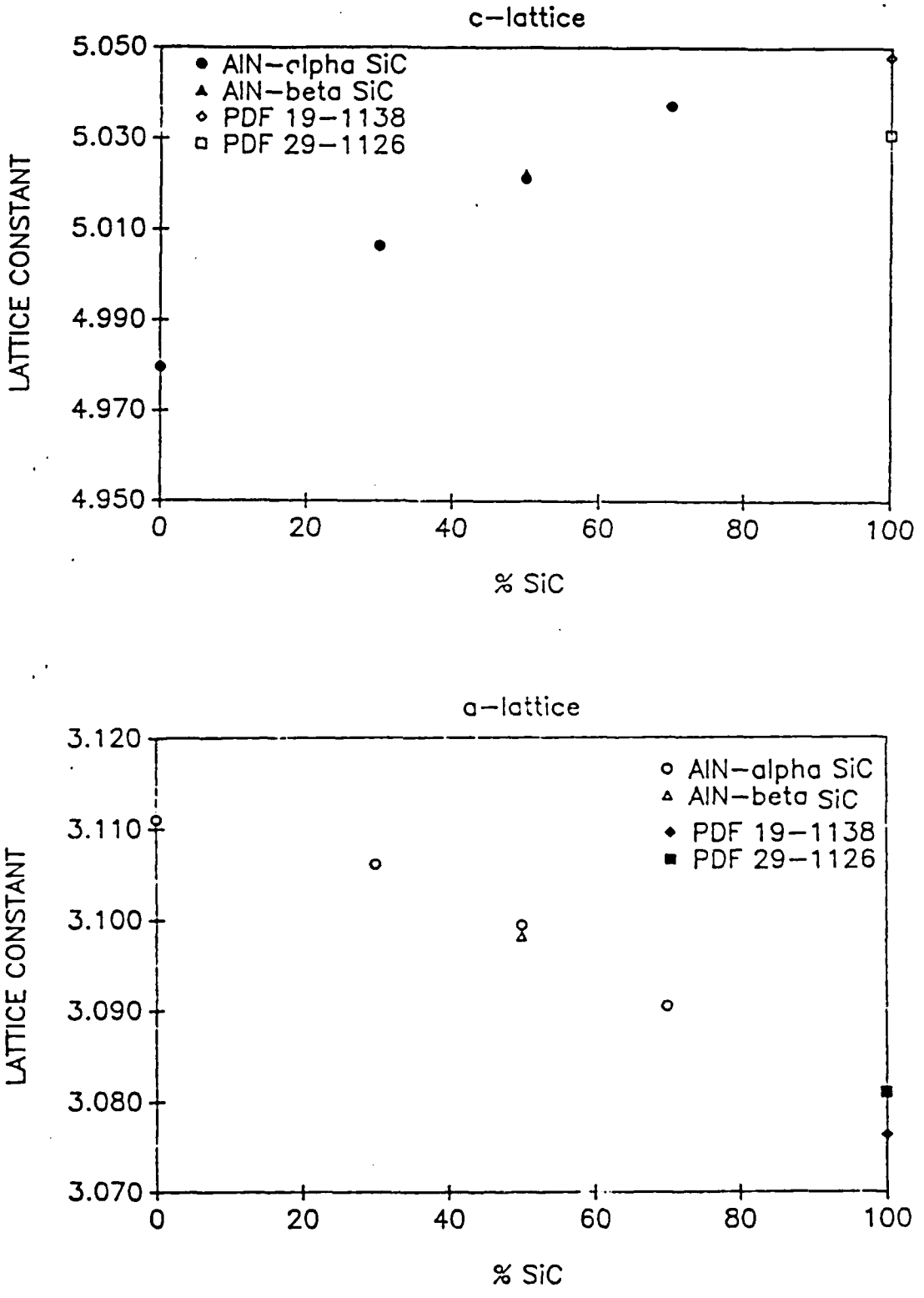

Figure 10 Lattice parameters of SiC-AlN alloys as a function of SiC content

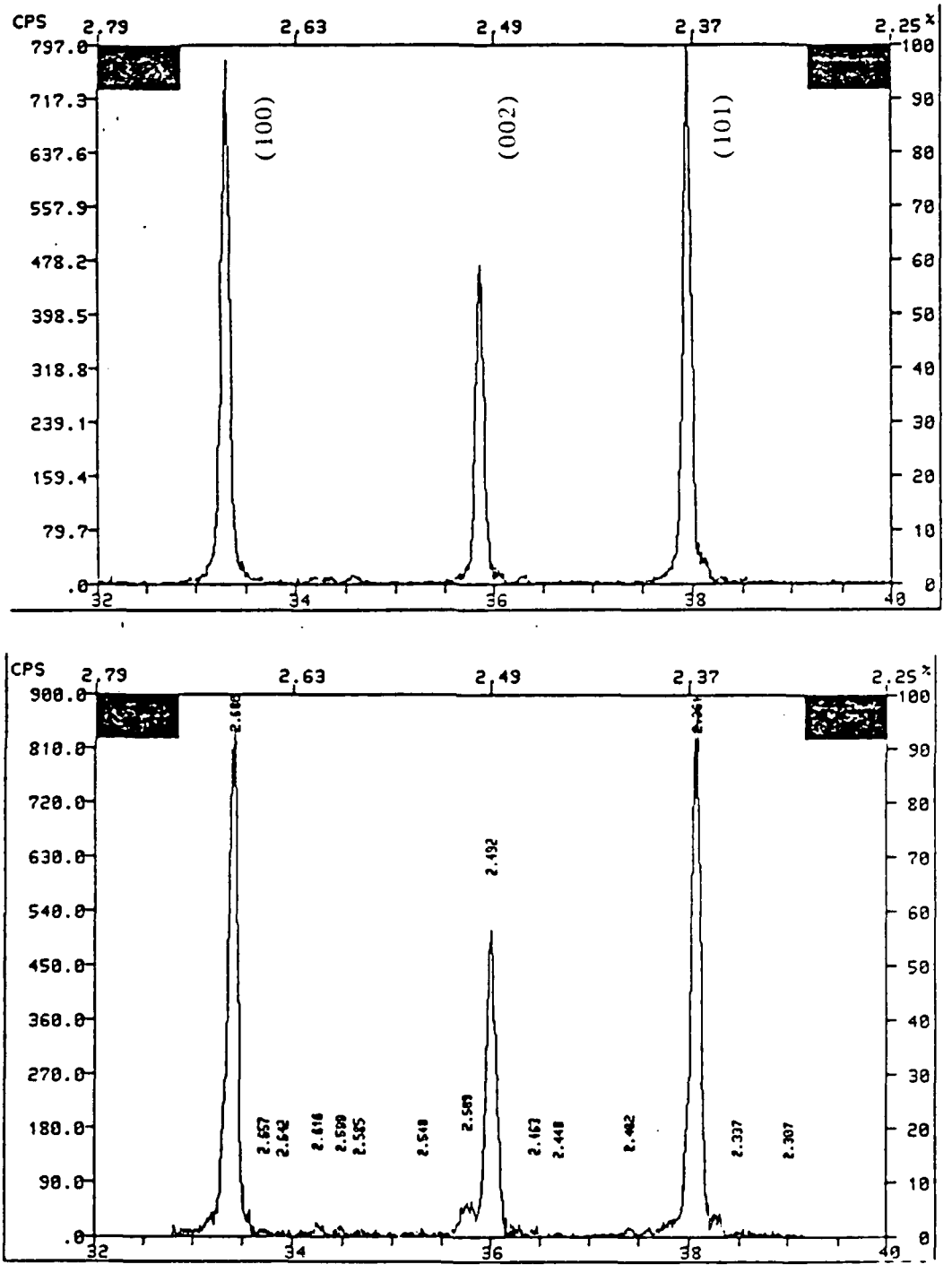

(a)

Figure 11 XRD patterns of alloys before and after annealing at 1860°C for 96 hr (a) 73Y2

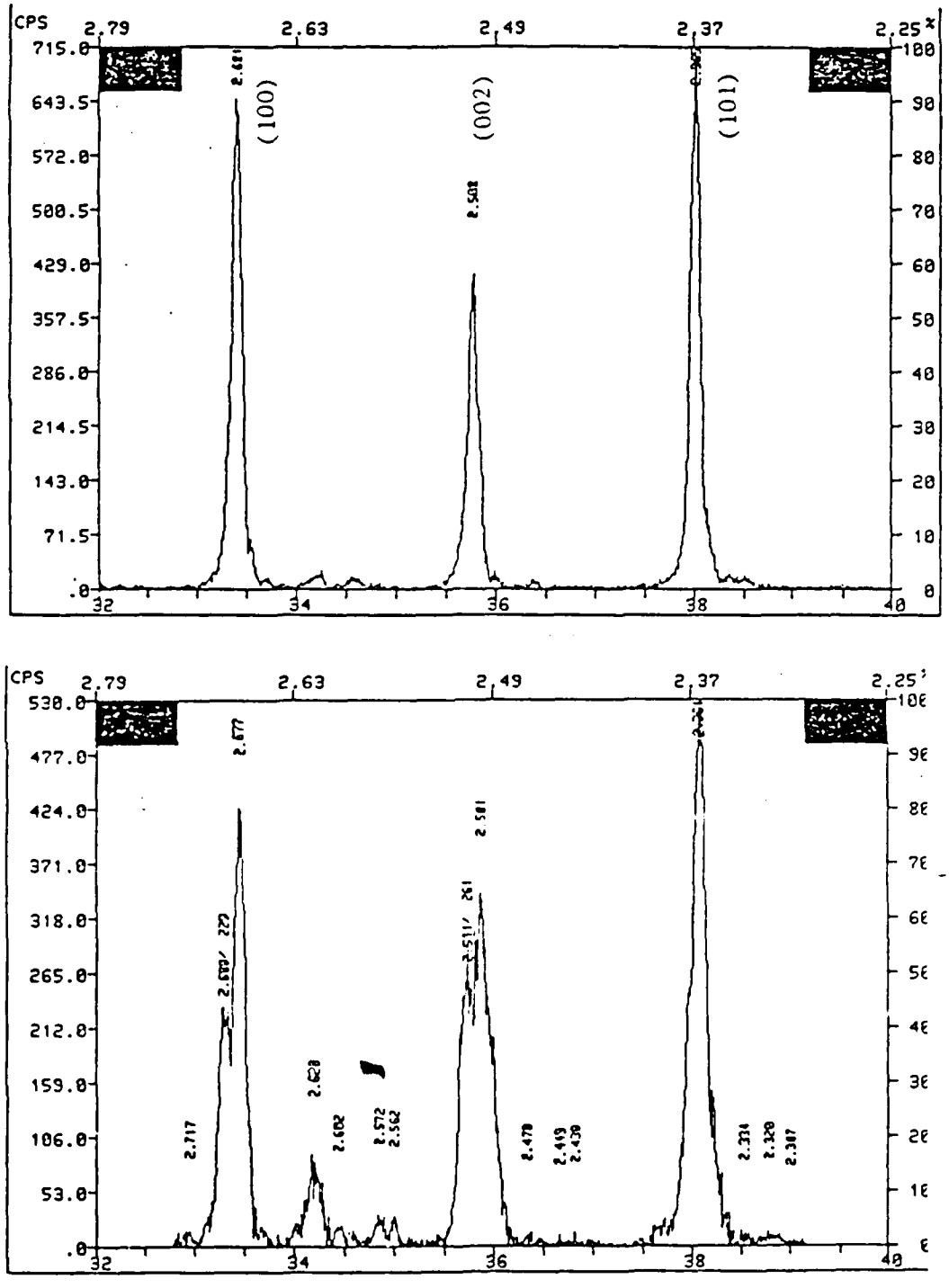

(b)

Figure 11 XRD patterns of alloys before and after annealing at 1860°C for 96 hr (b) AY2

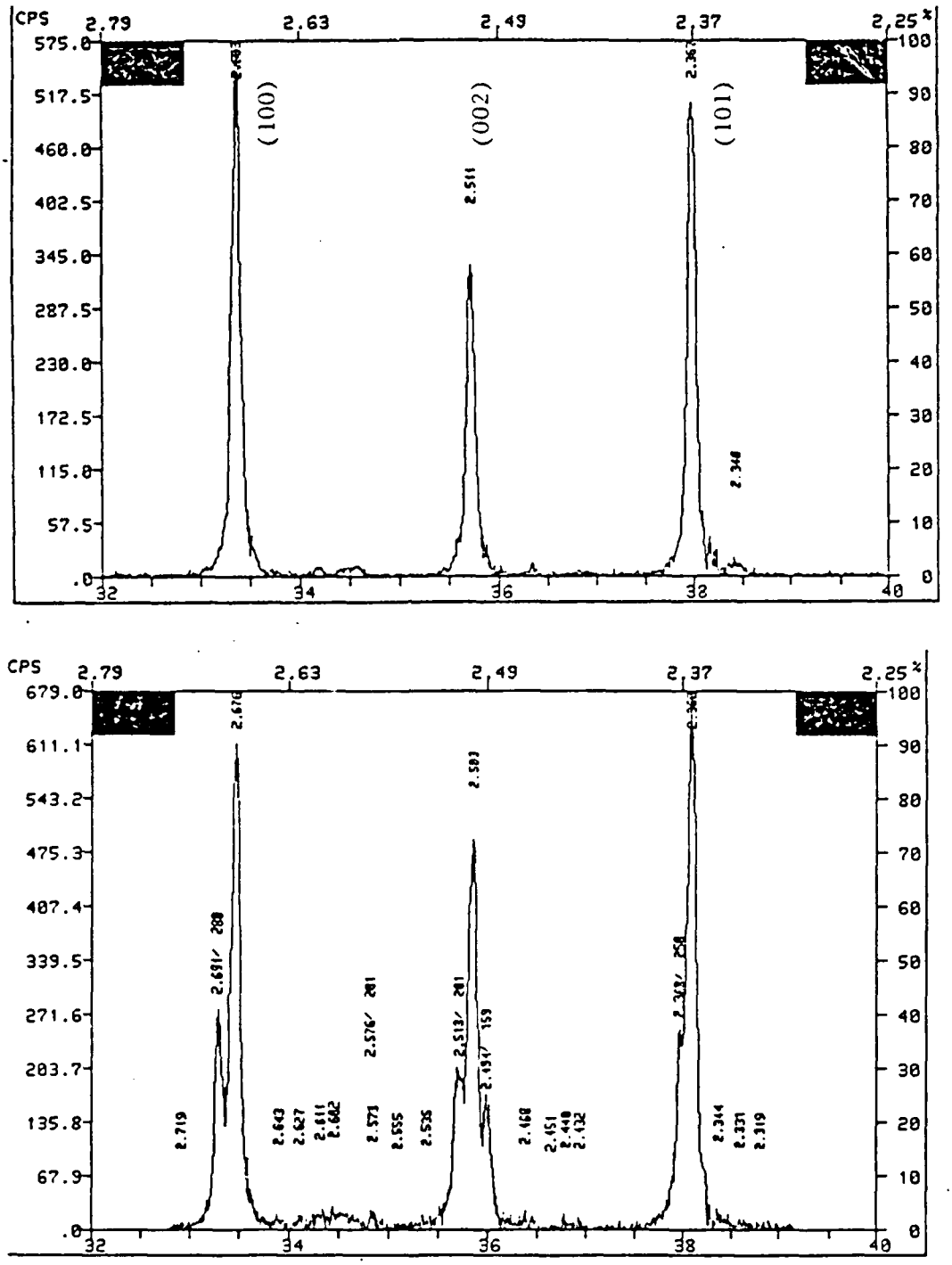

Figure 11 XRD patterns of alloys before and after annealing at 1960°C for 96 hr (c) SBY4

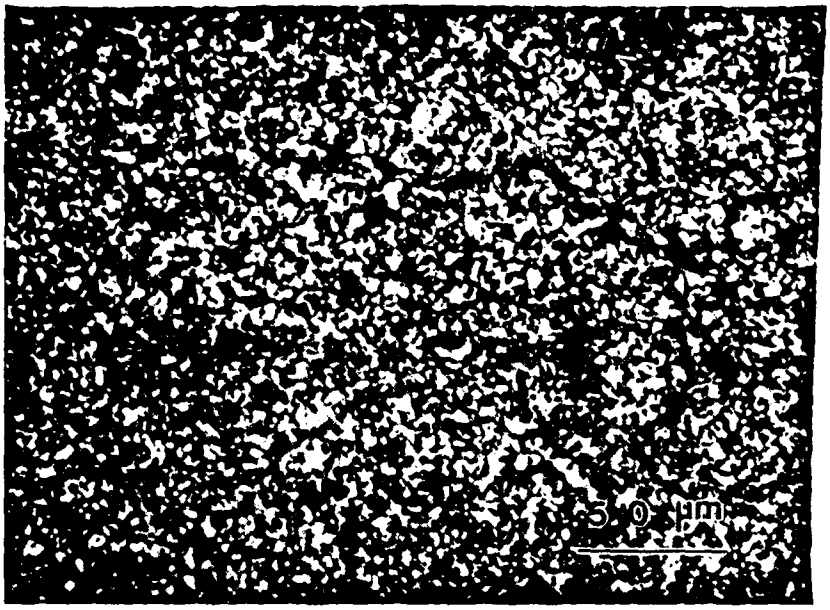

Figure 12 Optical micrograph of SBY4 showing 3 - 5 um grain size

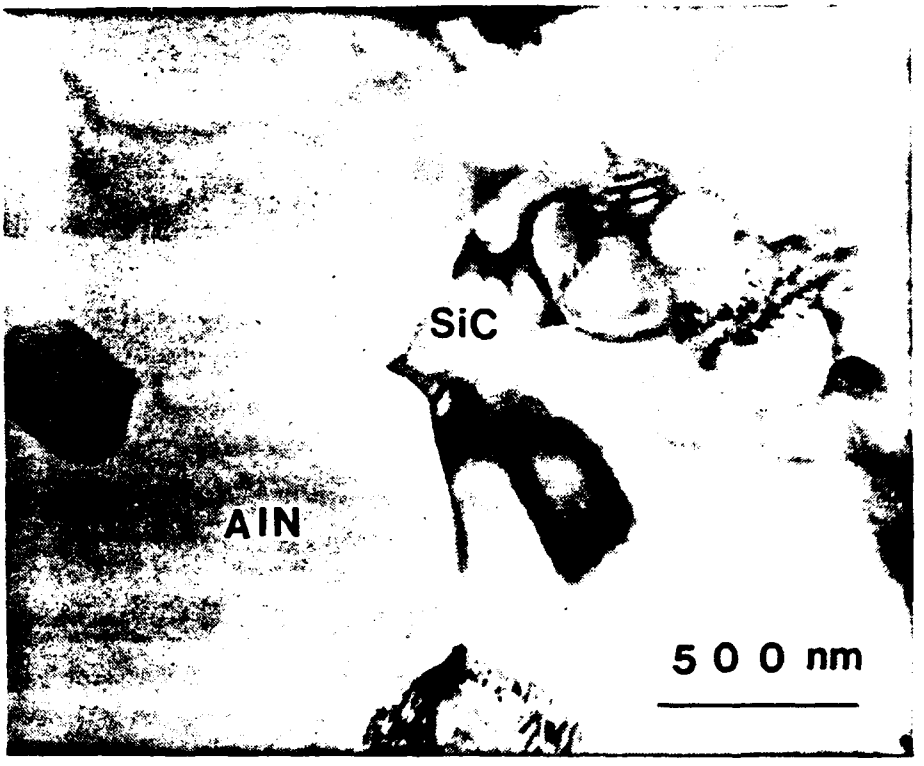

Figure 13 AY4 after sintering at 2100°C for 1 hr (a) TEM micrograph showing large AlN-rich grains and small SiC-rich grains

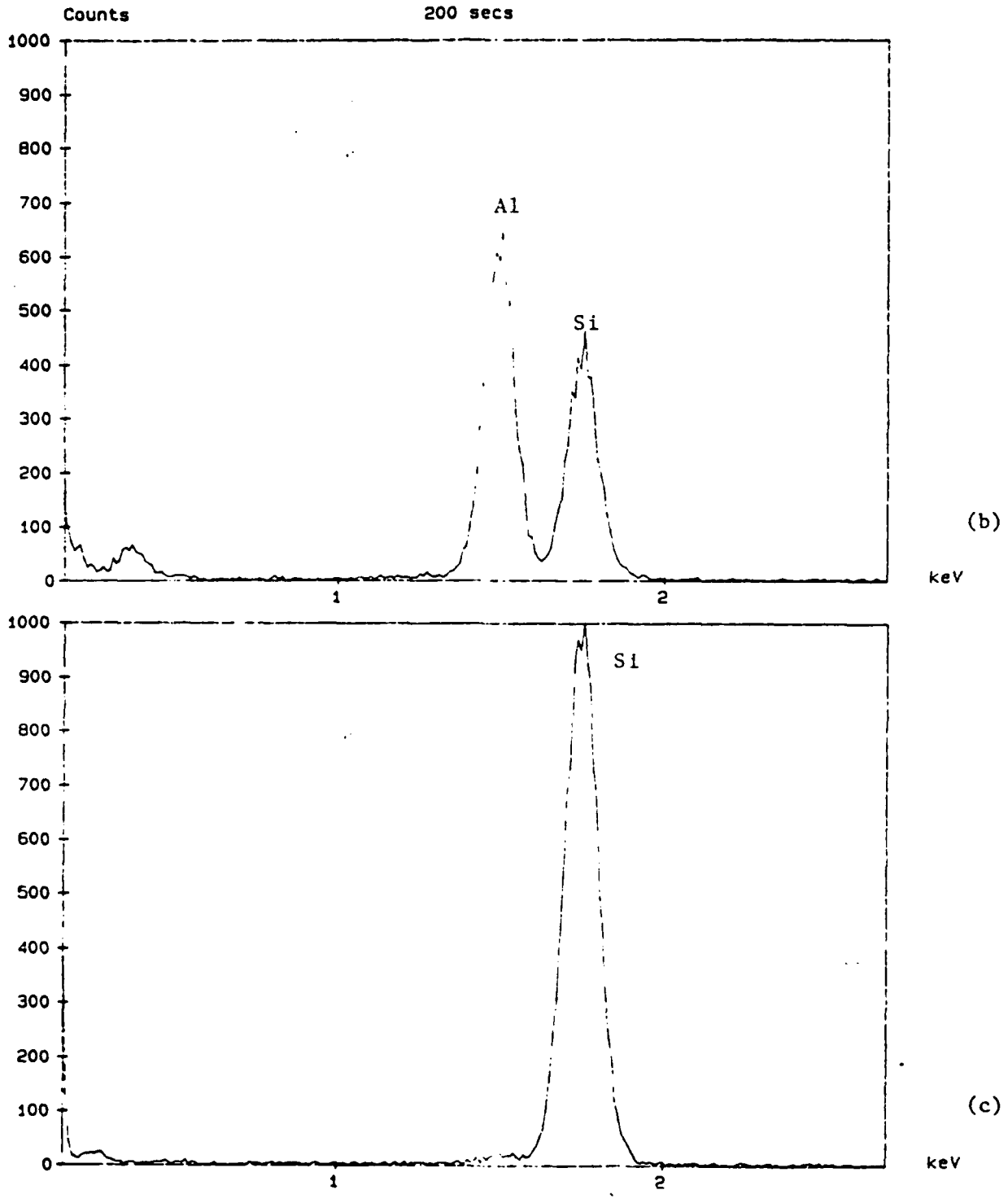

Figure 13 AY4 after sintering at 2100°C for 1 hour (b) EDS results on the large grains, (c) EDS on the small grains

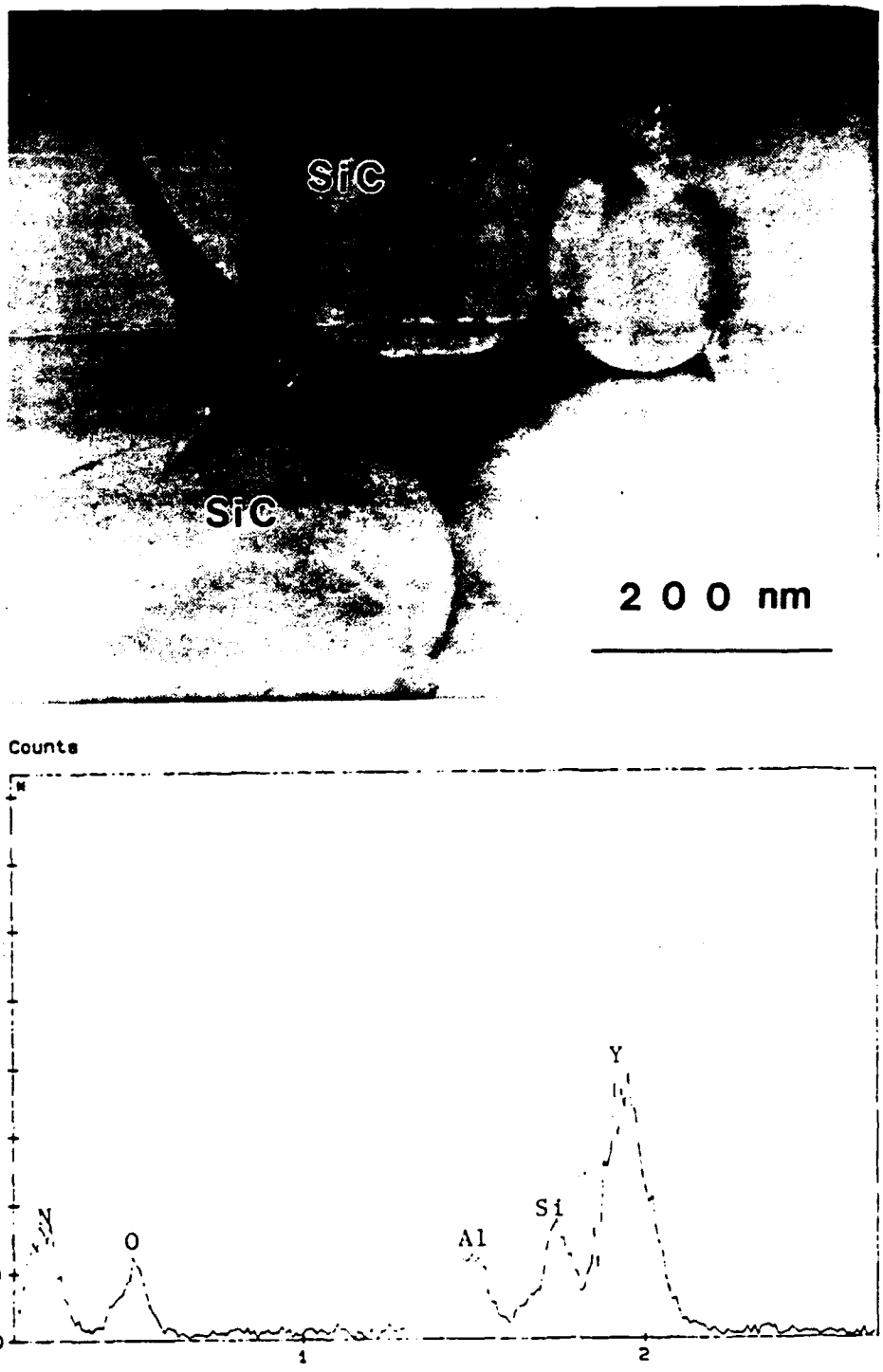

Figure 14 The SiC-rich area and grain boundary phase (a) TEM micrograph (b) EDS result on the grain boundary phase

Figure 15 TEM micrograph of AY2 after solid solution treatment at 2225°C

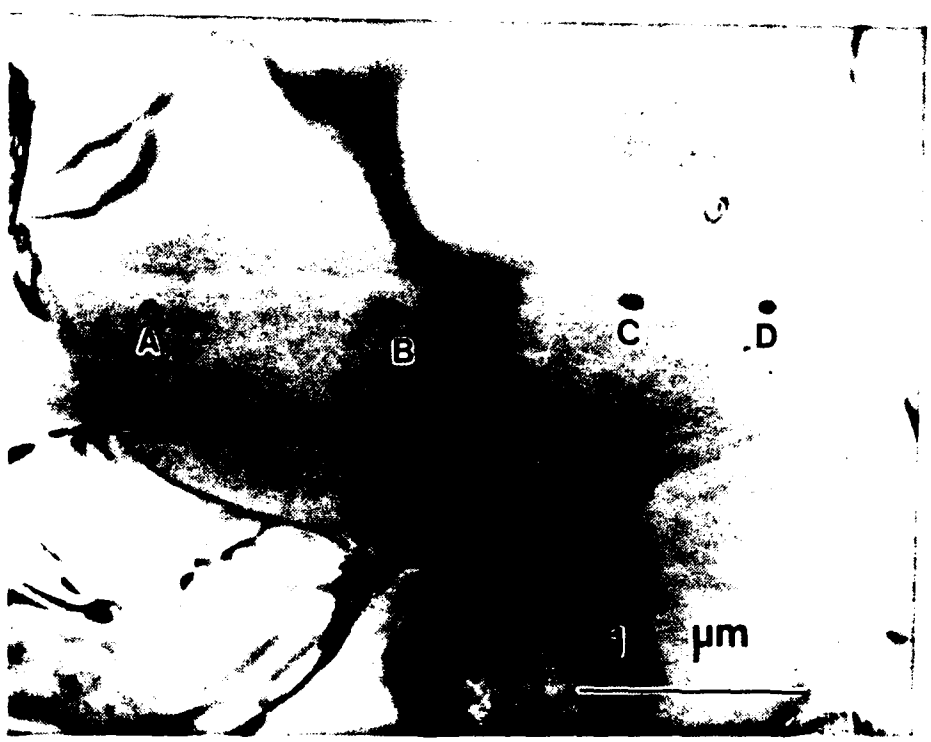

Figure 16 AY2 after solid solution treatment at 2225°C (a) TEM micrograph marked A,B,C and D showing the position for EDS analysis

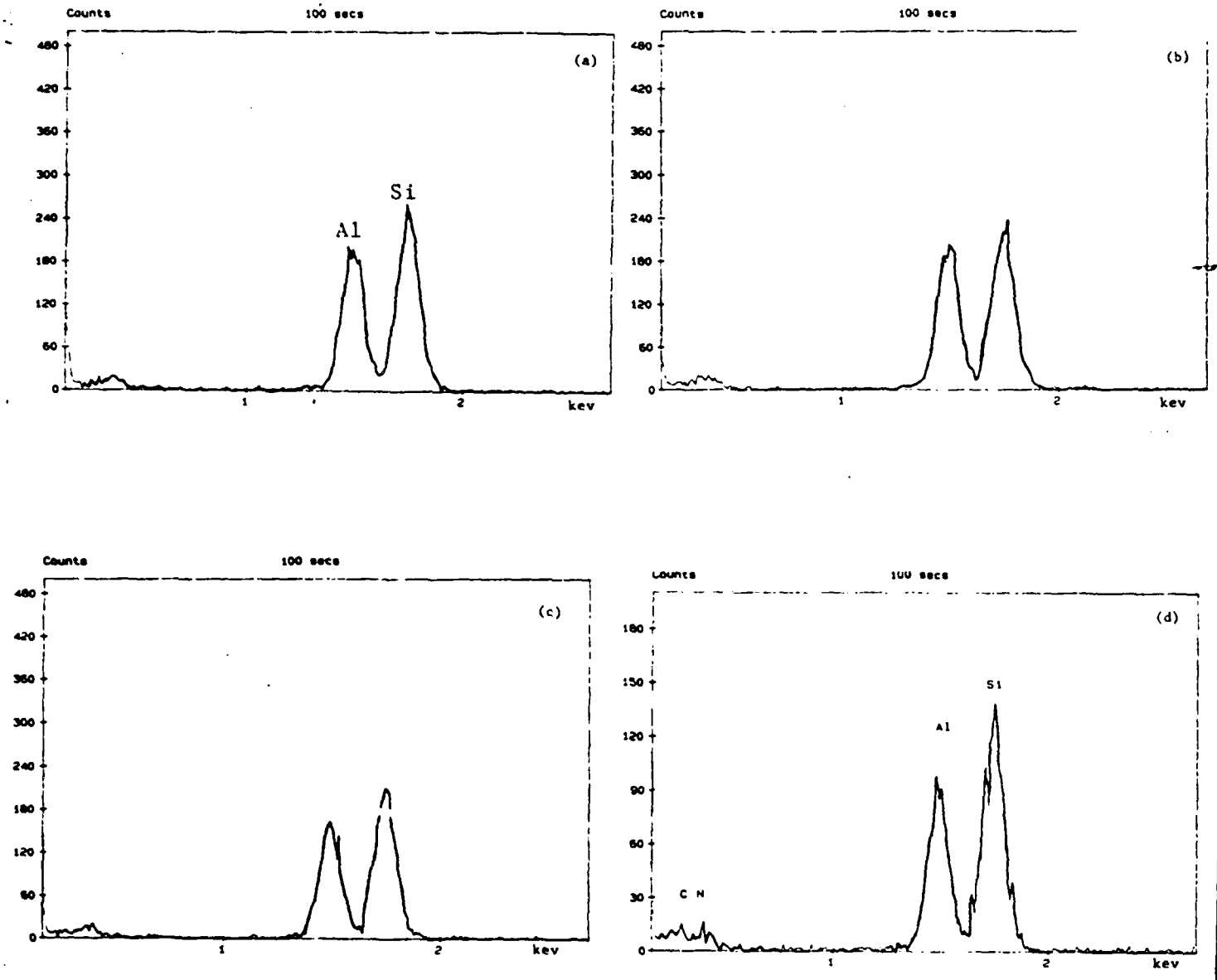

Figure 16 AY2 after solid solution treatment at 2225°C (b) EDS results

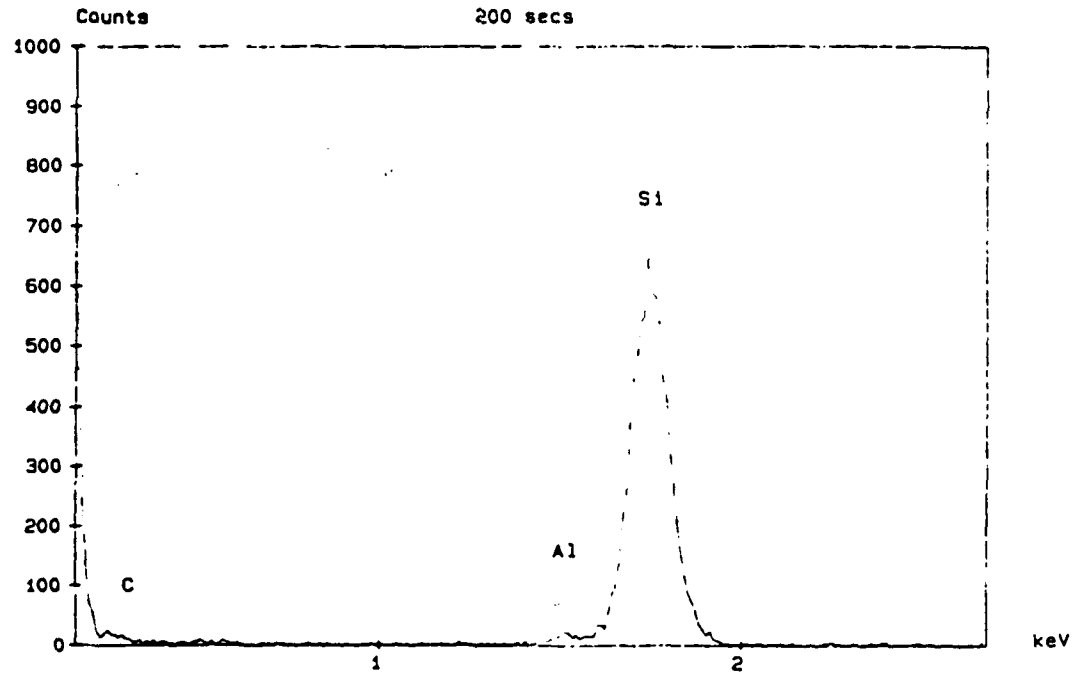

Figure 17 SiC particle trapped inside the SiAlCN grain (a) TEM micrograph (b) EDS result on the SiC particle

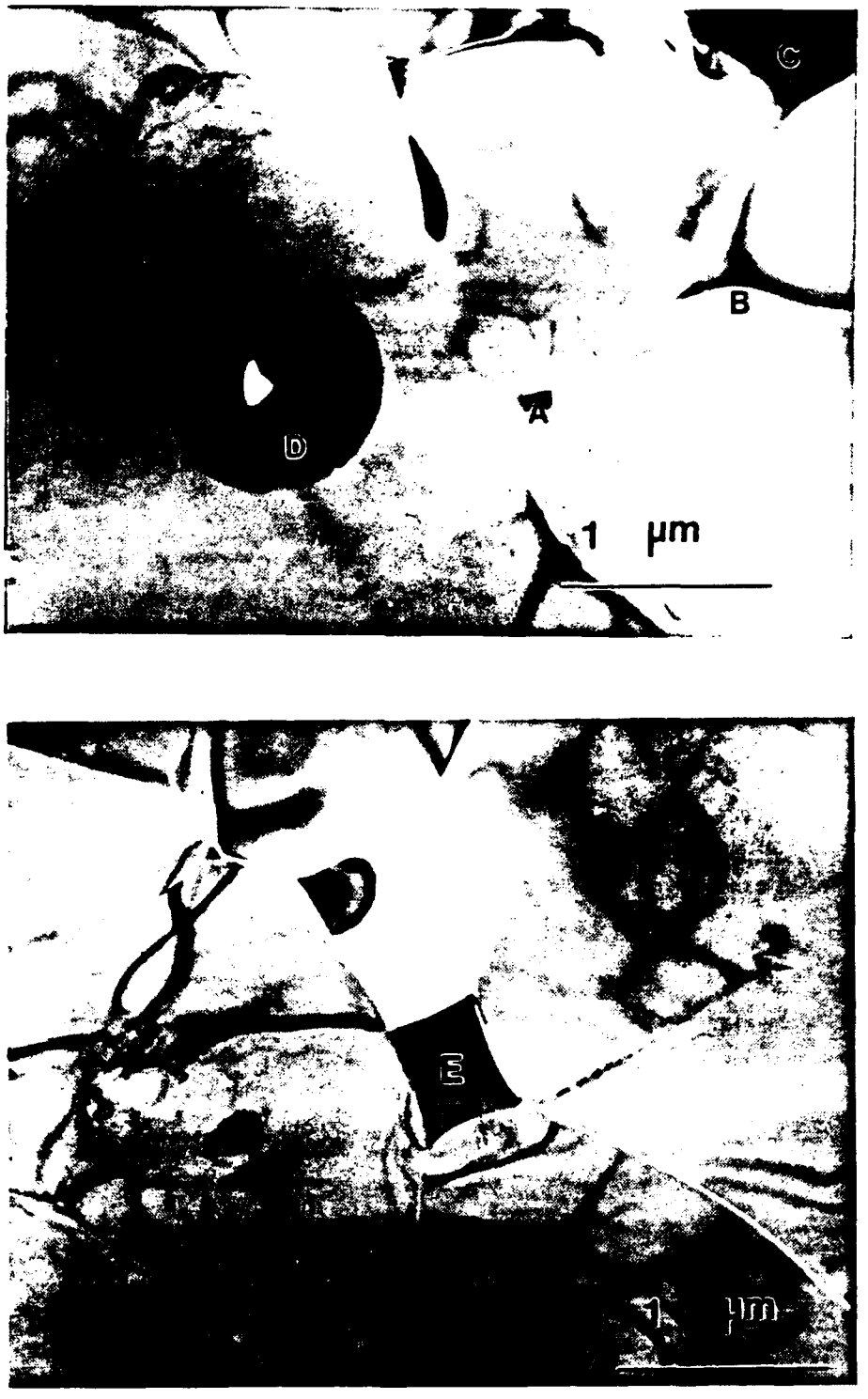

Figure 18 TEM micrographs showing different grain boundary phases in the AY2 after solid solution treatment at 2225°C

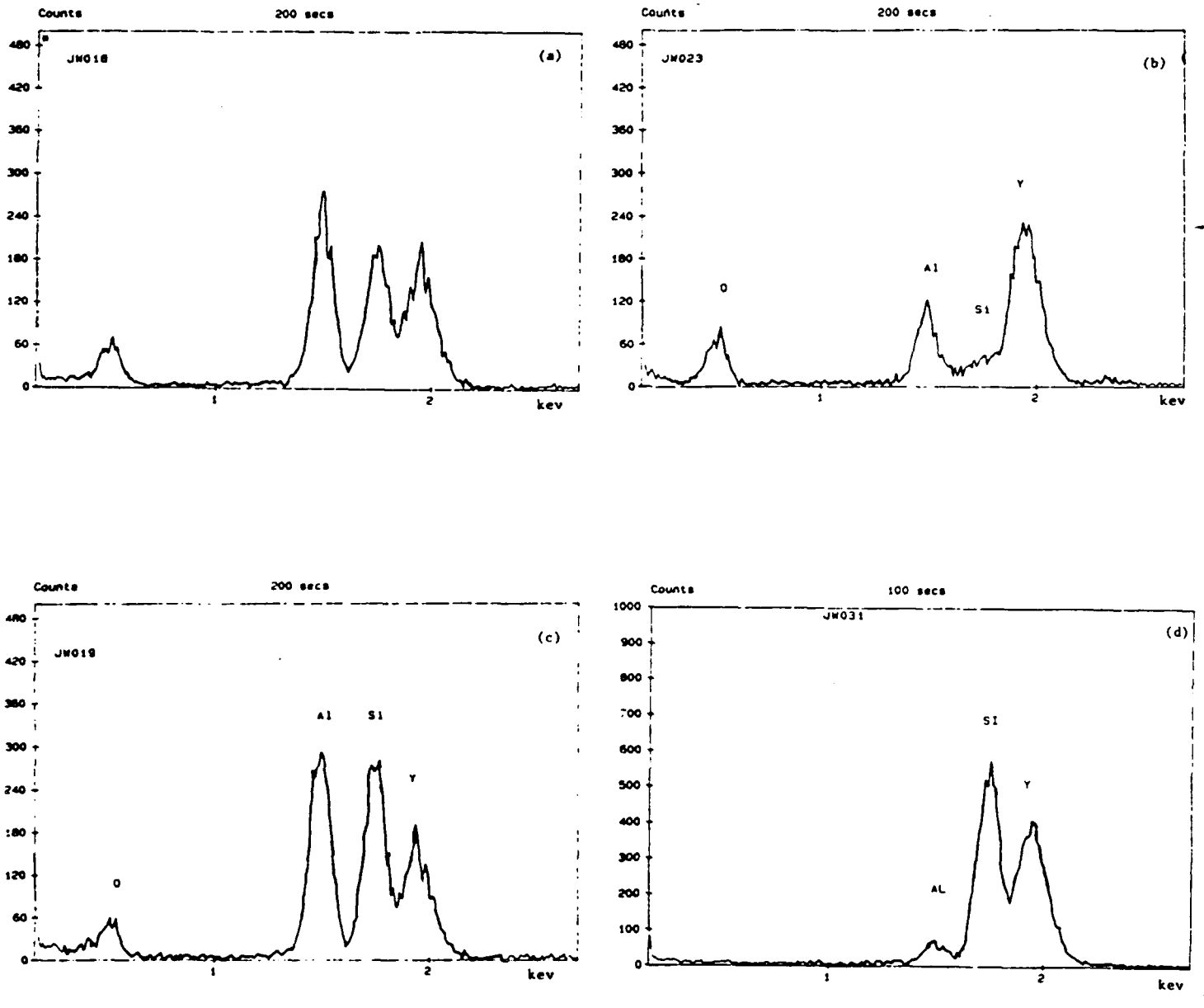

Figure 19 EDS results of grain boundary phase as marked in Figure 18 (a)area A , (b) area B, (c) area C, (d) area D

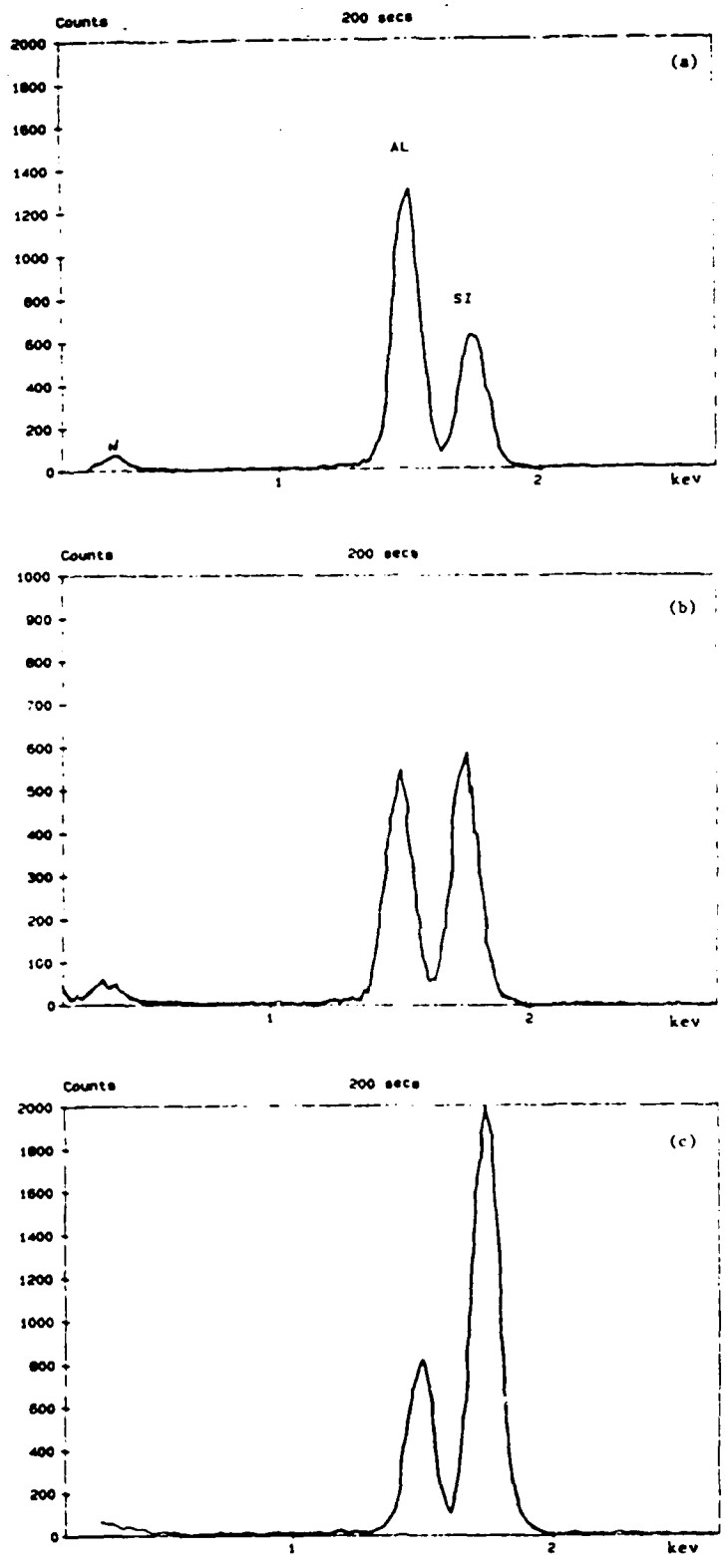

Figure 20 EDS results showing different ratio of Al/Si on the (a) 73Y2, (b) Y2, (c) 37Y2

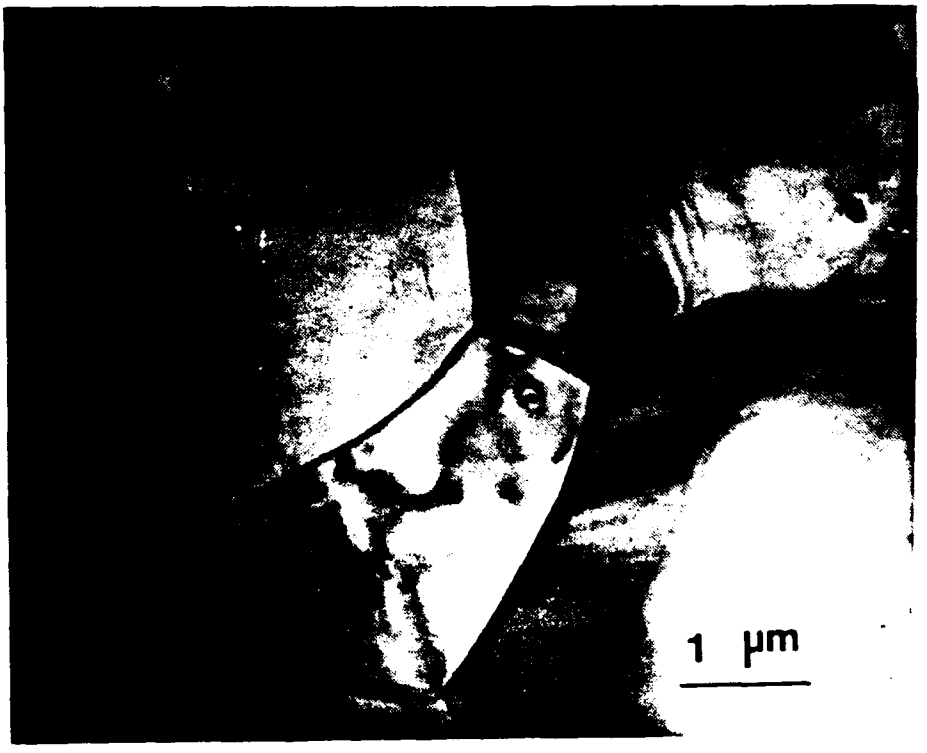

Figure 21 TEM micrograph of 73Y2 after annealing at 1860°C for 24 hr, showing clean grain boundary and some grain boundary phase and SiC particles were trapped inside the SiAlCN grains

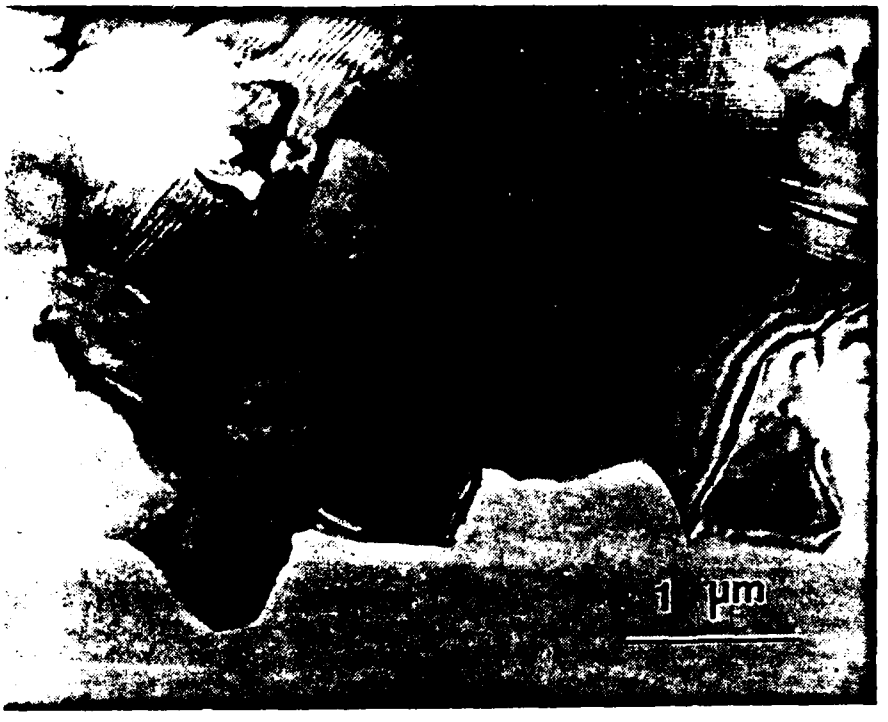

Figure 22 TEM micrograph showing duplex structure of AY2 after annealing at 1860°C for 96 hr

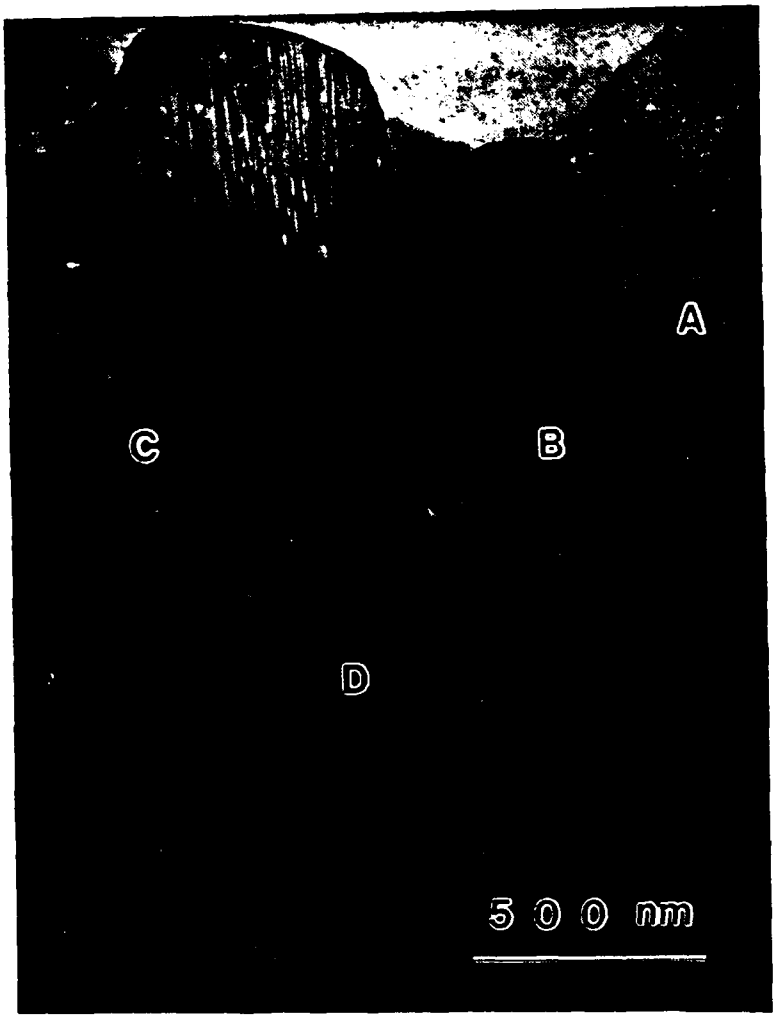

Figure 23 (a) High magnification of TEM micrograph showing duplex microstructure composed of equiaxed grains with modulate structure and elongated grain with heavy faulting

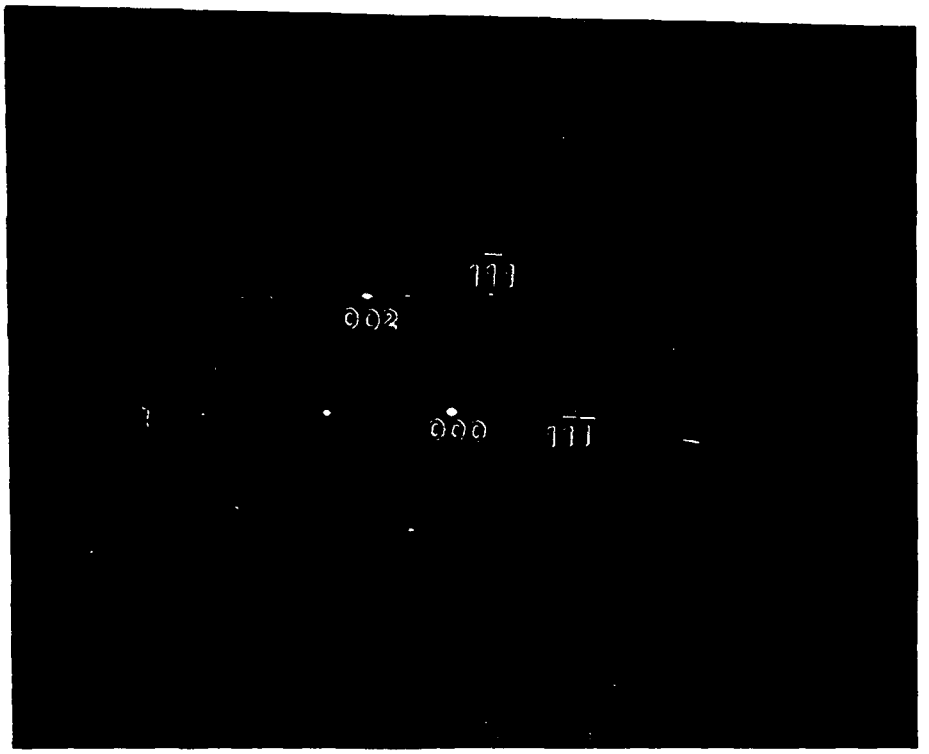

(c)

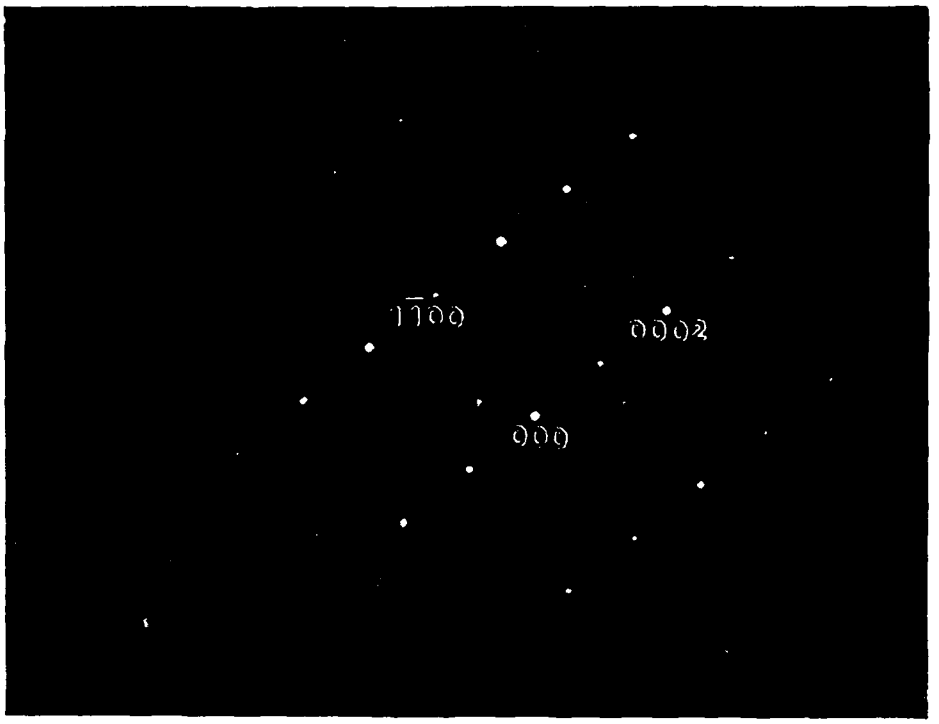

(b)

Figure 23 (b) Diffraction pattern of equiaxed grains at $[11\bar{2}0]$ zone showing 2H structure and the satellite peaks corresponding to the modulate structure c) Diffraction pattern of the elongated grain at $[110]_c$ zone showing 3C structure and the streaks corresponding to the heavy faulting

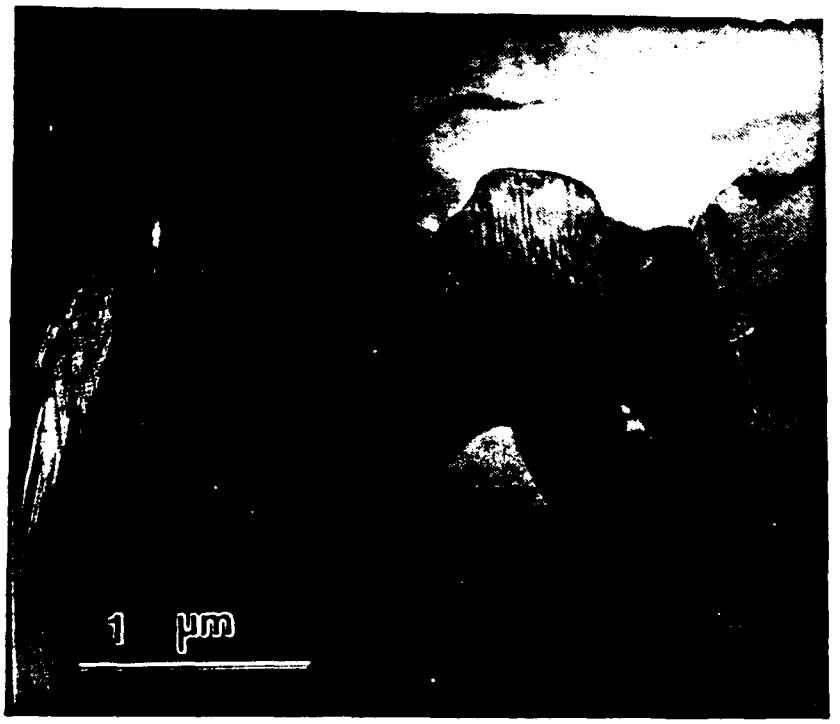

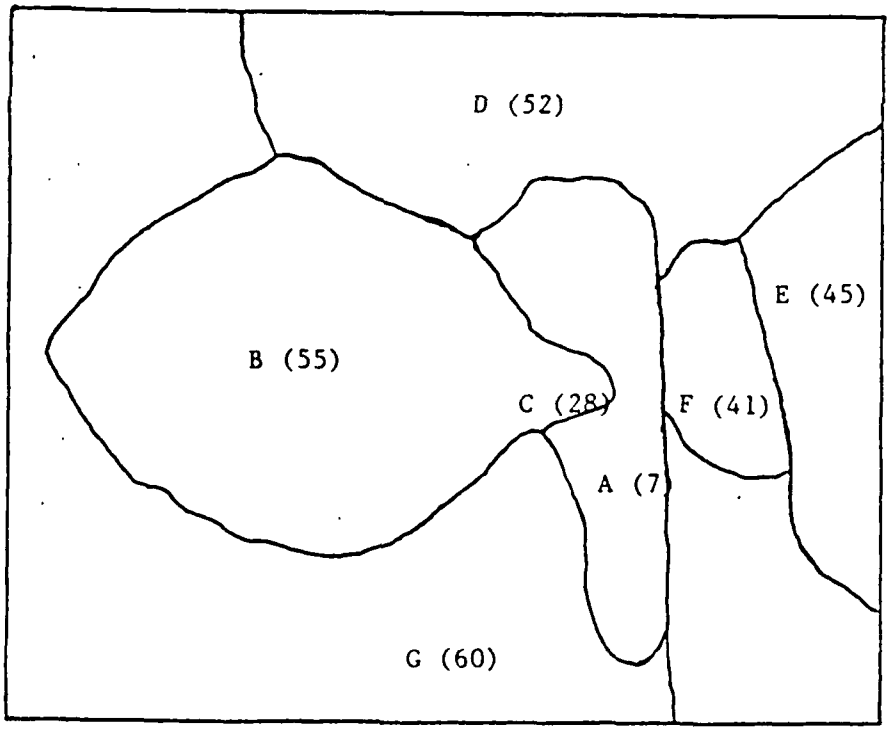

Figure 24 Duplexed microstructures of Figure 23 (a) Low magnification of Figure 23, (b) EDS results showing the AlN content in these areas

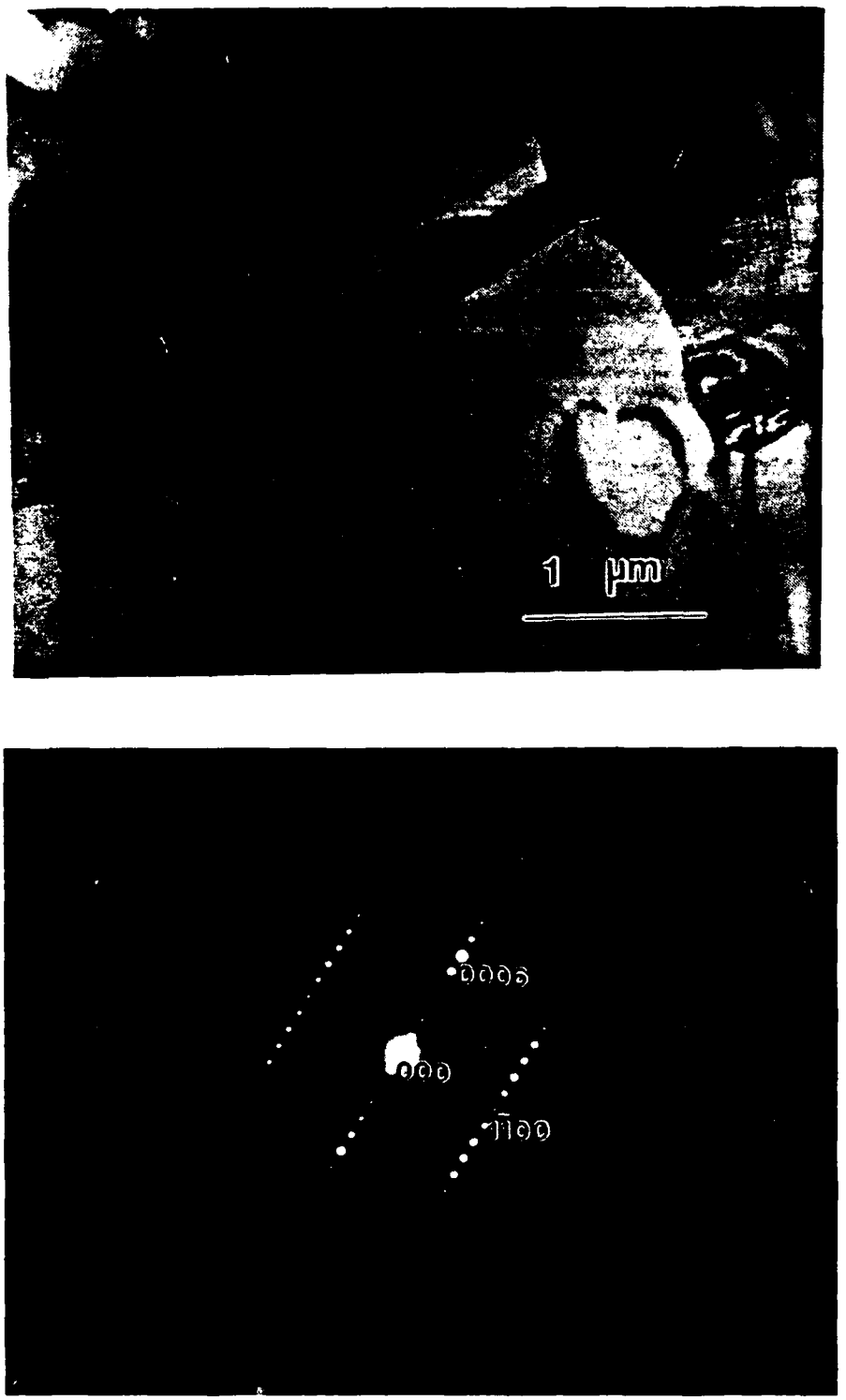

Figure 25 The 6H elongated grain surrounded by 2H equiaxed grains (a) TEM micrograph, (b) Diffraction pattern of the elongated grains at [11$\bar{2}$0] zone showing 6H structure

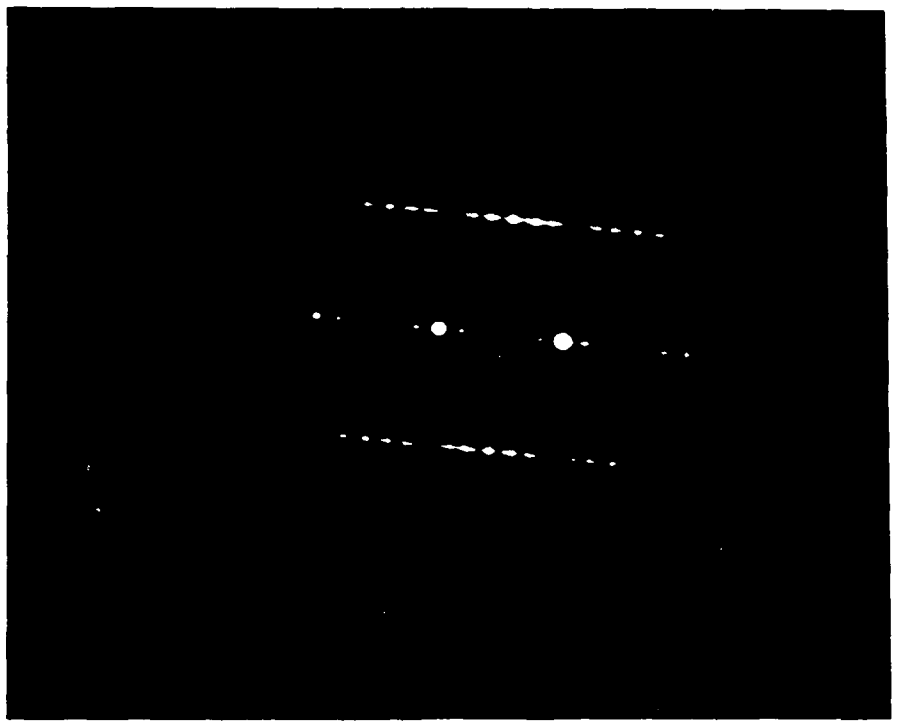

Figure 26 (a) TEM micrograph showing elongated grains having other polytype with heavy faulting (b) Diffraction pattern of the grain with heavy faulting

Figure 27 TEM micrograph of 37Y2 after annealing at 1860°C for 48 hr, showing a lot of elongated grains

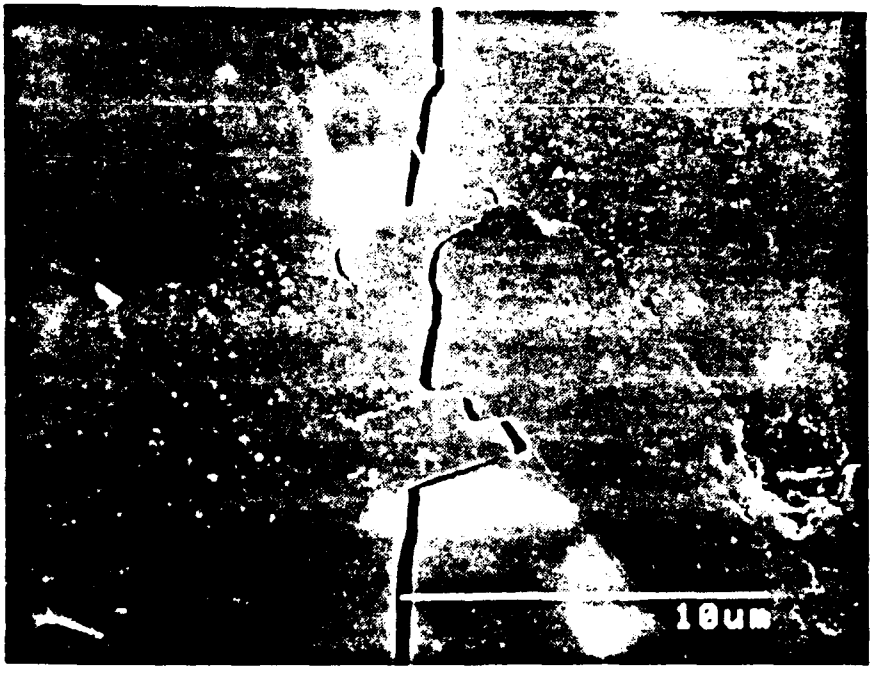

Figure 28 Crack-deflection of the elongated grains of the SiC-AlN alloys

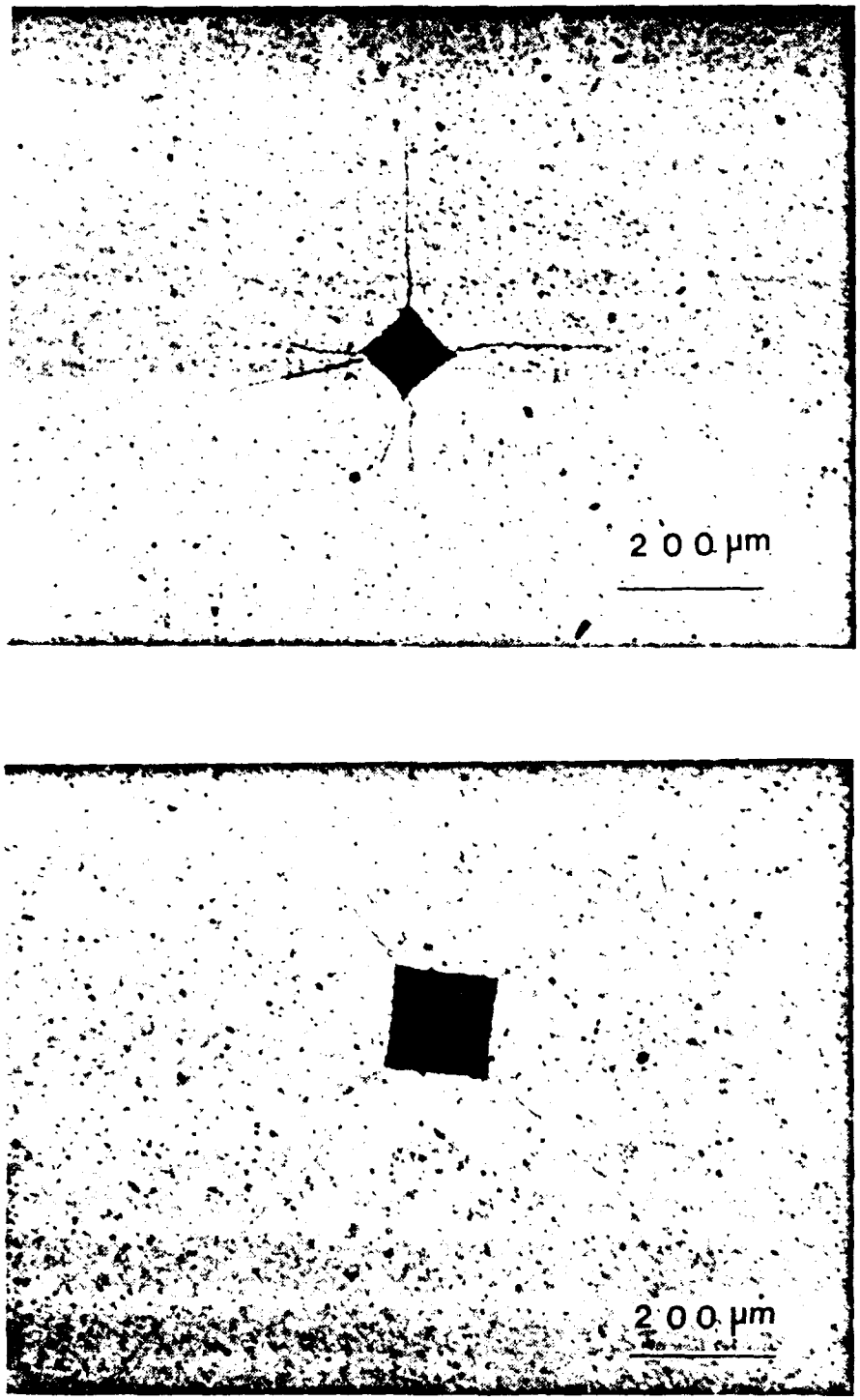

Figure 29 Optical micrograph showing the indentations and the resulting cracks on the (a) pure SiC, (b)pure AlN

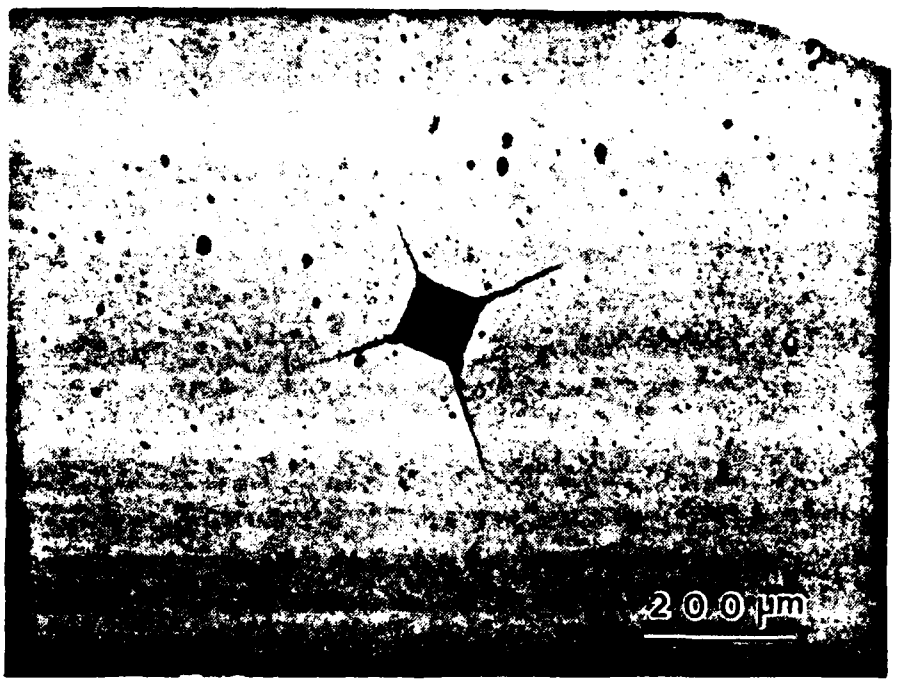

Figure 29 Optical micrograph showing the indentation and the resulting cracks on the (c) 37Y2

PUBLICATIONS

Because of the limited time available during Phase I of this research, the several papers which evolved from this research have not yet been published. The papers to be submitted for publication are listed below.

1. Ran-Rong Lee and Wen-Cheng J. Wei, "Fabrication of SiC-AlN Ceramic Alloys with Duplex Microstructure," to be submitted to the Journal of the American Ceramic Society.

2. Ran-Rong Lee and Wen-Cheng J. Wei, "Microstructure and Phase Transformation in the SiC-AlN Ceramic Alloys," to be submitted to the Journal of the American Ceramic Society.

3. Wen-Cheng J. Wei, Ran-Rong Lee, and James D. Hodge "Effects of Oxide Additives on the Sintering of AlN-SiC Composites," to be submitted to the Journal of the American Ceramic Society.

4. Camden Hubbard, Ran-Rong Lee, Wen-Cheng J. Wei, " XRD Investigation of SiC-AlN Solid Solution," to be submitted to the International Center of Diffraction Data.

INTERACTIONS

The following presentations will be given at upcoming conferences.

1. Wen-Cheng Wei, Ran-Rong Lee, and James D. Hodge "Effects of Oxide on the Sintering of AlN-SiC Composites" will be presented at the 91st American Ceramic Society Annual Meeting, Indianapolis, Indiana, April 23-27, 1989.

2. Ran-Rong Lee "Fabrication of High Temperature SiC-AlN Ceramic Alloys with Duplex Microstructure" will be presented in the First Ceramic Science and Technology Congress, Anaheim, CA, Oct.31-Nov. 3, 1989.

3. Camden Hubbard, Ran-Rong Lee, and Wen-Cheng J. Wei "XRD Investigation of SiC-AlN Solid Solution" will be presented at the Denver X-ray Conference, Denver, CO, Aug.2-Aug.4,1989.

Interaction with other laboratories

Part of the research was performed by Ceramics Process Systems' researchers on advanced and special instruments which were made available at the High Temperature Research Laboratory (HTML) at Oak Ridge National Laboratory (ORNL). Thanks are due to the committee of the User Center at HTML which allowed us to use their advanced analytical equipment. Special thanks are due to the following personnel who assisted us in the operation of the instruments, especially to Dr. C. Hubbard, Mr. B. Cavin, and Ms K. More.

PATENT DISCLOSURE

A patent application stemming from this research will be filed. DD Form 882 for the report of inventions is shpown on the following page.

REPORT OF INVENTIONS AND SUBCONTRACTS

(Pursuant to "Patent Rights" Contract Clause) (See Instructions on Reverse Side)

Form Approved OMB No. 0700-0260 Expires Feb 28 1987

1a NAME OF CONTRACTOR/SUBCONTRACTOR	c CONTRACT NUMBER	2a NAME OF GOVERNMENT PRIME CONTRACTOR	c CONTRACT NUMBER	3 TYPE OF REPORT (X one)
Ceramics Process Systems	F49620-88-C-0104			a INTERIM [X] b FINAL
b ADDRESS (Include ZIP Code)	**d AWARD DATE (YYMMDD)**	**b ADDRESS (Include ZIP Code)**	**d AWARD DATE (YYMMDD)**	**4 REPORTING PERIOD (YYMMDD)**
840 Memorial Drive Cambridge, MA 02139	88/18/07			a FROM 88/08/01 b TO 89/01/31

SECTION I - SUBJECT INVENTIONS

5 "SUBJECT INVENTIONS" REQUIRED TO BE REPORTED BY CONTRACTOR/SUBCONTRACTOR (If "None" so state)

a NAME(S) OF INVENTOR(S) (Last, First, Middle Initial)	b TITLE OF INVENTION(S)	c DISCLOSURE NO., PATENT APPLICATION SERIAL NO OR PATENT NO	d ELECTION TO FILE PATENT APPLICATIONS (1) United States (a) Yes	(b) No	(2) Foreign (a) Yes	(b) No	e CONFIRMATORY INSTRUMENT OR ASSIGNMENT FORWARDED TO CONTRACTING OFFICER (1) Yes	(2) No
Ran-Rong Lee Wen-Cheng J. Wei	Fabrication of silicon carbide-aluminum nitride ceramic alloys		X		X			X

f EMPLOYER OF INVENTOR(S) NOT EMPLOYED BY CONTRACTOR/SUBCONTRACTOR		g ELECTED FOREIGN COUNTRIES IN WHICH A PATENT APPLICATION WILL BE FILED	
(1) (a) Name of Inventor (Last, First, Middle Initial)	(2) (a) Name of Inventor (Last, First, Middle Initial)	(1) Title of Invention	(2) Foreign Countries of Patent Application
(b) Name of Employer	(b) Name of Employer	Fabrication of silicon carbide-aluminum nitride ceramic alloys	European Japan Korea
(c) Address of Employer (Include ZIP Code)	(c) Address of Employer (Include ZIP Code)		

SECTION II - SUBCONTRACTS (Containing a "Patent Rights" clause)

6 SUBCONTRACTS AWARDED BY CONTRACTOR/SUBCONTRACTOR (If "None" so state)

a NAME OF SUBCONTRACTOR(S)	b ADDRESS (Include ZIP Code)	c SUBCONTRACT NO (S)	d DLAR "PATENT RIGHTS" (1) Clause Number	(2) Date (YYMM)	e DESCRIPTION OF WORK TO BE PERFORMED UNDER SUBCONTRACT(S)	f SUBCONTRACT DATES (YYMMDD) (1) Award	(2) Estimated Completion

SECTION III - CERTIFICATION

7 CERTIFICATION OF REPORT BY CONTRACTOR/SUBCONTRACTOR (Not required if [ ] Small business or [ ] Non Profit organization (X appropriate box))

a NAME OF AUTHORIZED CONTRACTOR/SUBCONTRACTOR OFFICIAL (Last, First, MI)	c. I certify that the reporting party has procedures for prompt identification and timely disclosure of "Subject Inventions," that such procedures have been followed and that all "Subject Inventions" have been reported.	
b TITLE VICE PRESIDENT	d SIGNATURE	e DATE SIGNED